DEVELOPMENT OF LOW COST FILLER MATERIALS FOR WELDING
HIGH STRENGTH STEELS(U) OHIO STATE UNIV COLUMBUS DEPT
OF WELDING ENGINEERING R A BELL ET AL. 29 APR 84

UNCLASSIFIED N00014-81-K-0788

F/G 11/6

NL
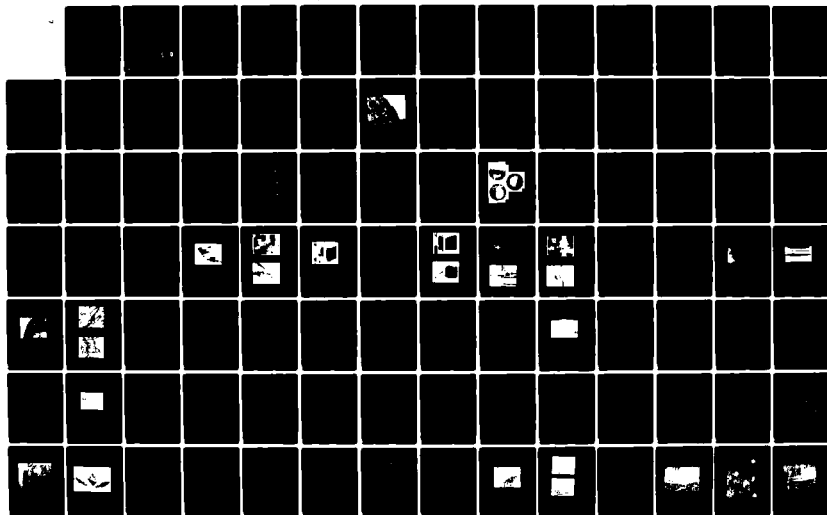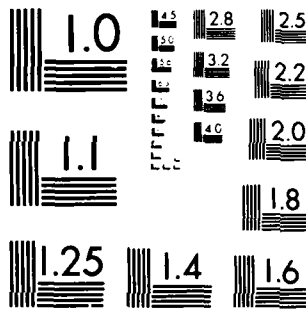
MICROCOPY RESOLUTION TEST CHART

NATIONAL BUREAU OF STANDARDS 1963 A

RF Project 762890/714158
Final Report

DEVELOPMENT OF LOW COST FILLER MATERIALS
FOR WELDING HIGH STRENGTH STEELS

Richard A. Bell, Denis E. Clark and David G. Howden
Department of Welding Engineering

For the Period
September 1, 1981 - December 31, 1983

DTIC
ELECTE
S JUN 0 4 1984
D
E

April 29, 1984

OSU **The Ohio State University
Research Foundation**
1314 Kinnear Road
Columbus, Ohio 43212

84 06 04 006

REPORT DOCUMENTATION PAGE		READ INSTRUCTIONS BEFORE COMPLETING FORM
1. REPORT NUMBER	2. GOVT ACCESSION NO. *A141 724*	3. RECIPIENT'S CATALOG NUMBER
4. TITLE (and Subtitle) DEVELOPMENT OF LOW COST FILLER MATERIALS FOR WELDING HIGH STRENGTH STEELS		5. TYPE OF REPORT & PERIOD COVERED Final Report 9/1/81-12/31/83
		6. PERFORMING ORG. REPORT NUMBER 762890/714158
7. AUTHOR(s) Richard A. Bell, Denis E. Clark and David G. Howden		8. CONTRACT OR GRANT NUMBER(s) N00014-81-K-0788
9. PERFORMING ORGANIZATION NAME AND ADDRESS The Ohio State University Research Foundation, 1314 Kinnear Road Columbus, Ohio 43212		10. PROGRAM ELEMENT, PROJECT, TASK AREA & WORK UNIT NUMBERS
11. CONTROLLING OFFICE NAME AND ADDRESS Office of Naval Research Department of the Navy Arlington, Virginia 22217		12. REPORT DATE April 29, 1984
		13. NUMBER OF PAGES 114
14. MONITORING AGENCY NAME & ADDRESS(if different from Controlling Office)		15. SECURITY CLASS. (of this report) Unclassified
		15a. DECLASSIFICATION/DOWNGRADING SCHEDULE

16. DISTRIBUTION STATEMENT (of this Report)

Approved for public release; distribution unlimited.

17. DISTRIBUTION STATEMENT (of the abstract entered in Block 20, if different from Report)

18. SUPPLEMENTARY NOTES

19. KEY WORDS (Continue on reverse side if necessary and identify by block number)

HY-130 steel, Welding (weld), Quenched + Tempered, Gas Metal Arc (GMAW),
Shielded Metal Arc (SMAW), Submerged Arc (SAW), Filler Materials, Weld Pool
Mixing, Weld Metal Synthesis

20. ABSTRACT (Continue on reverse side if necessary and identify by block number)
HY-130 is a quenched and tempered steel designed for high strength and
good toughness in the as-welded condition. The welding consumables, however,
are fairly expensive and the available sources limited. A study was conducted
to determine the feasibility of synthesizing the desired composition in the
weld pool using the Shielded Metal Arc (SMAW), Gas Metal Arc (GMAW), and
Submerged Arc (SAW) welding processes. This was accomplished by feeding two
commercially available materials into the weld pool in appropriate proportions.
(continued)

DD FORM 1473 1 JAN 73   EDITION OF 1 NOV 65 IS OBSOLETE

Block 20 (Abstract) - Continued

In the SMAW and SAW deposits adequate mixing of the two materials was achieved. Some inhomogeneities were observed in the GMAW deep penetration finger. This slight lack of mixing could be improved through further process development. Weldments produced with all three processes met the yield strength and elongation requirements for 140 filler materials. Dynamic tear tests conducted on submerged arc weldments came close to meeting the requirements while weldments produced with the other processes were somewhat lower. This was thought to be due to higher than allowed residual element levels and could be improved through optimization of starting material compositions. The techniques developed in this program have shown potential for obtaining weld metals of specific compositions for high strength steels at reduced cost.

FINAL TECHNICAL REPORT

on

DEVELOPMENT OF LOW COST FILLER MATERIALS

FOR WELDING HIGH STRENGTH STEELS

by

Richard A. Bell, Denis E. Clark and David G. Howden

The Ohio State University
Department of Welding Engineering
190 West 19th Avenue
Columbus, Ohio 43210

April 29, 1984

FOREWORD

TABLE OF CONTENTS

             Final welding parameters used for producing mechanical
             properties test plates

LIST OF FIGURES

LIST OF TABLES

INTRODUCTION

The work reported was carried out for the U.S. Navy, David Taylor Naval Ship Research and Development Center, Annapolis, MD. under contract N0016782RC00219/8-2-82 as part of an on going effort to develop improved materials and more economic fabrication methods for high strength steels. The program was directed towards the development of new methods of achieving weld metal compositions suitable for the fabrication of HY-130 steel plate. The technique involved mixing of two wires of different compositions in the welding zone in such proportions that an appropriate weld metal composition was synthesized during the welding operation. The welding processes investigated were:

> Gas Metal Arc Welding
> Submerged Arc Welding
> Shielded Metal Arc Welding

For the first two processes, the arc was maintained between a main wire and the weld pool while a second wire of high alloy was added to the system. For the SMAW process, special composite electrodes were manufactured using either a conventional core wire with the second high alloy material placed along the surface in ribbon form or a tubular core "wire" with the high alloy inserted in wire form.

The potential advantages of this development were threefold:

Economy.
: For the GMAW and SAW processes, an 80 percent reduction in the cost of filler wire could be realized if commercially available wires could be used instead of custom made E-140S material.

Versatility.
: There are a limited number of qualified suppliers of welding materials for HY-130 and none for SAW. Successful development of the presently considered techniques could provide alternative suppliers. In addition, the two wire technique would allow subtle changes of composition to be made simply by adjusting the proportions of the two wires.

Quality.
: It was suspected that a more homogenous SMAW weld metal could be achieved if alloying elements were added to the pool in "metallic" form rather than via the coating as is the conventional practice.

The program involved a demonstration of the feasibility of the technique, fabrication of test weldments and an evaluation of mechanical properties for each of the processes.

BACKGROUND

The background is divided into several sections dealing with the nature of the steel, it's weldability, filler materials available,economics and considerations for alternative approaches to filler metal development.

HY-130 Steel

HY-130 is nominally a 0.1C-5Ni-0.5Cr-0.5Mo quenched and tempered steel with a yield strength of 130,000 psi. and good toughness, designed for welding and to be used in the as-welded condition in thicknesses up to 4 inches. It's metallurgical structure is primarily martensitic although at greater thickness some bainite is present in the microstructure.   Table 1 shows the HY-130 base plate composition specification (1).   Since the mechanical properties of the steel are achieved by quenching and tempering, welding conditions such as preheat and heat input must be carefully controlled to avoid any deterioration of properties in the weld heat affected zone (HAZ). The relatively low level of carbon in the steel helps to maintain the hardness in the weld HAZ reasonably low although the total alloy content of the steel is relatively high and, hence, it's hardenability.

Weld Filler Metals for HY-130

The filler metal composition is similar, but not identical, to that of the base metal, since the weld metal is designed to achieve a yield strength level of 135,000 psi. in the as-welded condition.

The filler metal compositions have been optimized for each individual process based on expected dilution by the base metal and the heat input of the welding process (and hence the cooling rate). Since, in at least two of the processes (GMAW and SMAW), a successful composition has been established, the present work used these as target compositions. However, the mechanics of the filler metal development of the present investigation differs from the traditional approach.

Conventionally, the GMAW wire composition is specified to be in such a range that, when diluted by the base metal, a suitable composition results. Apart from minor losses due to vaporization or oxidation (transfer inefficiency) the deposited weld metal composition can be predicted.

The SMAW situation is different, however. In this case, the core wire consists of a low carbon steel and the desired alloying elements are added to the flux covering on the rod. As the flux melts during welding it frees the alloying elements which dissolve in the molten weld pool. The flux formulation is, therefore, quite complex and manufacturers normally maintain the information proprietary. The SMAW electrode is classified based on the composition of the deposited weld metal rather than that of the electrode.

There are currently two commercially available filler metals in solid wire form for use in GMAW and GTAW welding of HY-130, Linde 140S and Airco AX140. As can be seen from Table 2, they achieve their properties with somewhat different compositions, the Linde wire being higher in Ni and lower in Cr

3

TABLE 1.   SPECIFIED COMPOSITION FOR HY-130 BASE PLATE
MIL-S-24371A --SHIPS
(Weight Percent)

Element	Percentage, max unless range is shown
C	0.12
Mn	0.60-0.90
P	0.01
S	0.01
Si	0.15-0.35
Ni	4.75-5.25
Cr	0.40-0.70
Mo	0.30-0.65
V	0.05-0.10
Ti	0.02
Cu	0.25

TABLE 2. COMPOSITIONS OF MCKAY 14018, AIRCO AX-140,
AND LINDE L-140 ELECTRODES FOR WELDING HY-130
(Weight Percent)

Element	Airco AX-140	Linde L-140	McKay (typical)
C	0.05-0.09	0.06-0.12	0.054
Mn	1.90-2.20	1.50-1.90	0.98
Si	0.25-0.45	0.35-0.45	0.25
P	0.01 max	0.01 max	0.009
S	0.01 max	0.01 max	0.004
Ni	2.0-2.5	2.3-2.9	3.53
Cr	1.0-1.25	0.65-0.90	0.59
Mo	0.5-0.6	0.70-1.0	0.87

Note---Airco data for Dorschu and Lesnewich 1964
       Linde technical data, 1983
       McKay data from pad analysis

and Mn than the Airco. MIL. spec for solid welding wire reflects ranges of composition whch encompass both these compositions.(2) The sole qualified electrode for SMAW of HY-130 is the Teledyne-McKay E14018. Its composition, also shown in Table 2, is again different, being higher in Ni than that of the solid wires. While not just any composition in the useful range can be expected to meet requirements, this variety of compositions indicates that there is considerable latitude in designing such a material.

Elemental Transfer

Weld metal composition is seldom identical with electrode composition. On the average, the weld deposit composition will be lower than the electrode composition. The ratio of this difference is known as the transfer efficiency. The electrode material is also diluted by the base material the weld melts into the deposit. This will cause either depletion or enrichment, according to the relative compositions.

Heuschekel (3) has measured transfer efficiencies for a number of welding processes, and states that preferential oxidation is the most common cause of reduced transfer efficiency. Transfer efficiency depends not only on the particular element involved, but also on the welding process and conditions. Filler materials for a given process must thus be enriched in elements with lower transfer efficiencies.

Filler metal sources in arc welding include the following:

1. Electrode wire
2. Base metal
3. Non-electrode wire
4. Metal powder:
    a. In electrode coating
    b. Under flux (Bulkwelding)
    c. Agglomerated with flux
    d. In tubular electrode

In consumable wire processes, the electrode wire generally contributes the bulk of the weld deposit, though base metal dilutions of up to 50% are common, and metal powder contributions can approach those of the electrode wire.

Weld Metal Homogeneity

There are several phenomena tending to produce inhomogeneities in the weld deposit:

Microsegregation

Macrosegregation

Incomplete mixing in a system with a heterogeneous source of
                                    filler material
The partially melted and unmixed zones of the base metal

Completely melted base metal subject to turbulent flow but
incomplete mixing

Microsegregation is the preferential inclusion or exclusion of solute elements at a solidification front in an alloy. It is the result of the change in solidus and liquidus temperatures brought on by the presence of the solute element, as explained by Flemings (4), which leads to segregation of alloying elements between solidifying dendrites or cells. Welds commonly solidify under conditions that produce dendritic or cellular structures (5), and the solute-enriched or solute-impoverished liquid is trapped locally rather than being carried along indefinitely as in plane-front solidification. The final result is local composition variation on the scale of the dendrites, which are much smaller than the grains. Assuming that the molten weld pool is homogeneous, microsegregation in any particular alloy systems, may be expected regardless of how the chemical composition of the pool was achieved.

Macrosegregation can normally be related to fluid flow conditions within the molten pool. Enriched or impoverished fluid is carried off and relatively large areas of a solidifying mass can vary substantially from the mean composition.

Incomplete mixing in a welding system that uses a heterogeneous filler material source has been known to cause weld metal composition heterogeneities, though practical processes are usually optimized to avoid this. Areas of melted but unmixed metal powder additions are sometimes found in the SAW Bulkwelding process (which increases deposition rates by using a layer of metal powder underneath the flux) at high levels of powder addition (see figures 1 and 2). Inclusions, identifiable by microprobe analysis as having come from the electrode coating, are seen in low-alloy steel SMAW, in which the core wire is mild steel and the alloying elements are contained in the electrode coating in the form of metal powders. Gouch and Muir (6) found them to be quite common in the first pass of pipeline welds, where the heat input is generally lowest.

Partially-melted and fully-melted but unmixed zones exist at the fusion line (5). Their presence can be demonstrated by selective etching (7). While these zones are too thin to have a large effect on mechanical properties, the thermal history of the area and the fact that weld metal chemical modifications do not reach them can make them a source of microcracks (ibid).

The GMAW process, with its homogeneous filler wire, avoids the direct deposit of off-composition areas. The high current density spray transfer process produces a "finger" penetration at the base of the weld, however, and this finger is associated with incomplete mixing between weld metal and base metal (8), porosity (9), and cracking (10). The first two problems are attributed to the faster solidification rate of the finger zone, while the cracking is attributed to its acute shape and consequent nonuniform stresses and heating. Considering that the present work relates to the addition of two filler wires for synthesis of weld metal composition, particular attention had to be paid to macrosegregational effects.

7
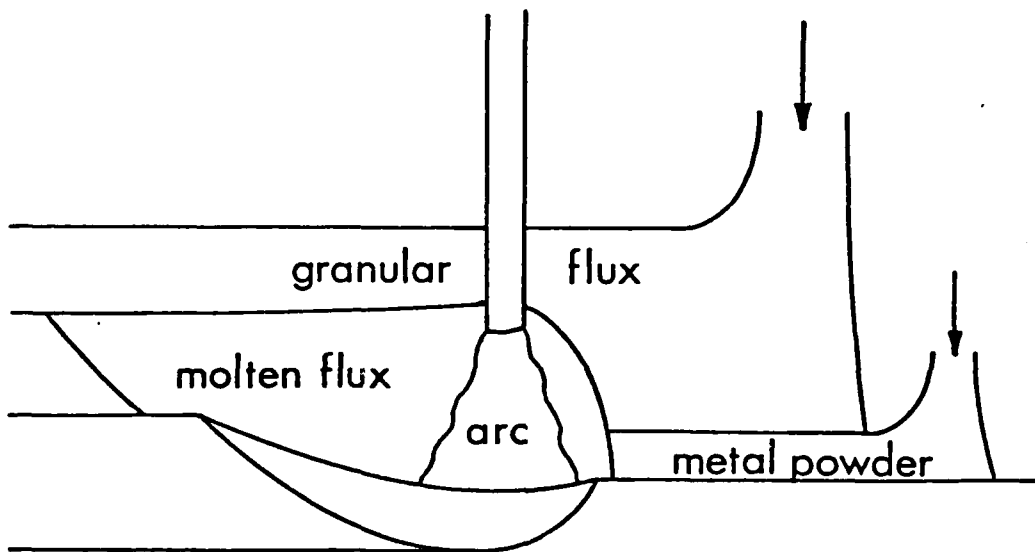
Figure 1. Schematic illustration of the Bulkwelding process.
This is a variation of the Submerged Arc Welding process in
which metal powder is added to increase the deposition rate.

8
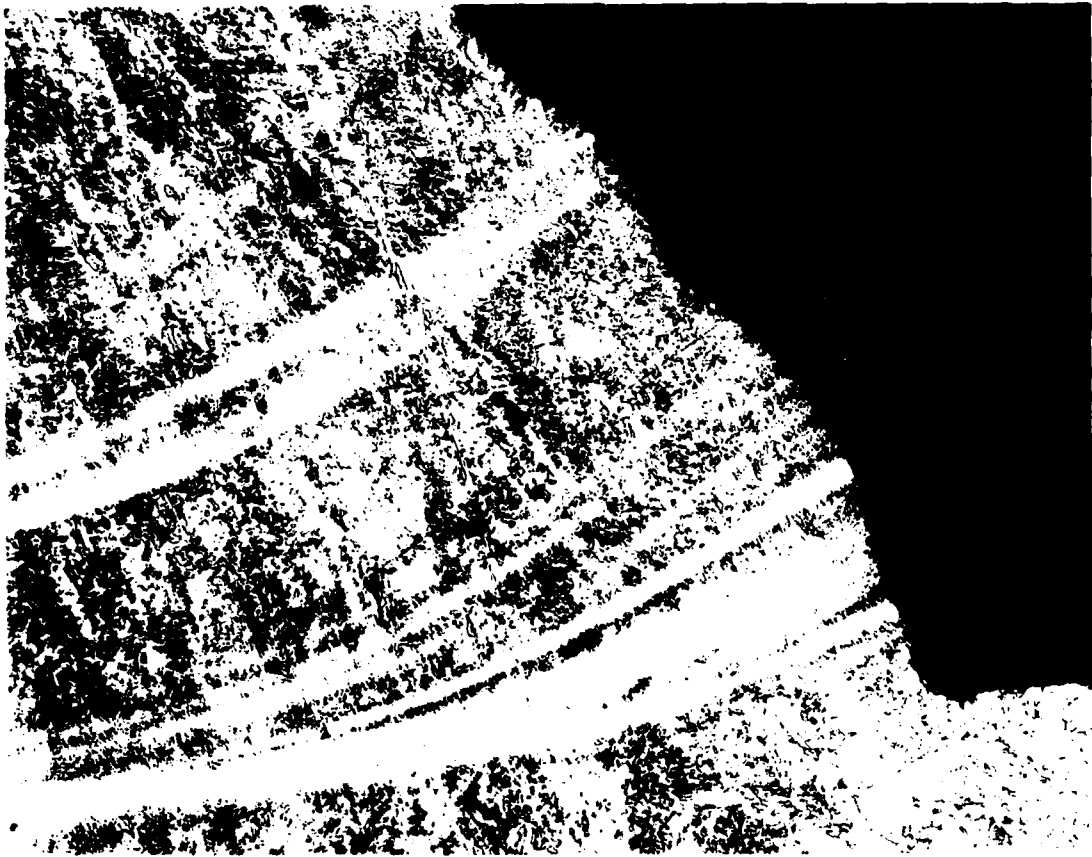
Figure 2. The toe of a Submerged Arc weld made with the Bulk-
welding process. The light etching bands are rich in iron
powder as a result of incomplete mixing.

9

Candidate Materials for the Secondary Wire

Secondary-wire alloy additions for synthesizing weld metals for HY-130 were evaluated by searching for candidate materials, calculating deposit compositions, developing welding procedures, and evaluating weld deposits for gross chemistry, homogeneity, and mechanical properties.

Since the object was to minimize the amount of alloyed material, the initial search for secondary wire candidate materials was restricted to commercial nickel-based alloys or iron-based alloys high in Ni, whose addition in amounts under 10% would achieve the required filler metal levels. The Ni:Cr:Mo ratio also had to be approximately correct for a commercial material to be considered, although it was anticipated that in later stages of the work this could be adjusted by using custom-made alloys. The search was made from the compositions listed in materials handbooks, alloy producer catalogs, and in consultation with alloy producers. Table 3 gives a list of the materials considered in detail. The main criteria for the primary wire were low cost, low residual elements, and carbon, manganese, and silicon levels appropriate to 140 ksi filler material.

Prediction of Weld Metal Composition for Gas Metal Arc
  and Submerged Arc Welding

Candidate materials that fit the above criteria were further evaluated by calculating their projected weld deposit chemistry.

The main and secondary wire together make up the entire deposit (not allowing for dilution). Factoring in relative densities, wire diameters, feed speeds, and transfer efficiencies produces the following equation:

$$C_{dep} = \frac{C_p(E_p)(IPM_p)(D_p)^2(\rho_p) + C_s(E_s)(IPM_s)(D_s)^2(\rho_p)}{(IPM_p)(D_p)^2(\rho_p) + (IPM_s)(D_s)^2(\rho s)}$$

where C_{dep} = deposit composition
       C_p = composition of primary wire in a particular element
       C_s = composition of secondary wire in a particular element
    ipm_p = feed speed of primary wire
    ipm_p = feed speed of secondary wire
       ρ_p = density of primary wire
       ρ_p = density of secondary wire
       D_p = diameter of primary wire
       D_s = diameter of secondary wire
       F^s = transfer efficiency of primary wire
       E^p_s = transfer efficiency of secondary wire

Except for the wire feed speeds, all of these terms are constant in a given two-wire system. This means that a plot of deposit composition versus percentage secondary wire added (which converts readily to wire feed ratios) produces a straight line for each element, having a y-intercept at the primary wire composition and a slope corresponding to the secondary wire composition. Inserting the specified deposit composition limits on the

TABLE 3. CANDIDATE MATERIALS EVALUATED FOR SECONDARY WIRE
(BAL. Fe UNLESS SPECIFIED)
(Weight Percent)

Material	Ni	Cr	Mo	Other
Hastelloy X	47	22	9	2 Co; .5 W
Incoloy 825	42	21.5	3	2.25 Cu
Hastelloy C-4	63	16	15.5	2 Co; .7 Ti
A-286	26	15	1.25	2 Ti
Incoloy 901	42.5	12.5	6	2.7 Ti
Inconel 625	61	21.5	9	3.6 Nb

abscissa and projecting onto the ordinate gives the appropriate mixture limits for each element; an overlapping zone will produce a deposit within the limits, while near misses can be estimated. Figures 3, 4 and 5 show how this was done in three wire systems for Ni, Cr, and Mo, the most important alloying elements in the HY-130 system.

Since previous work in secondary wire alloying was done in the SAW process using Linde 44B main wire and Hastelloy "X" secondary wire (11), this combination was the first investigated for GMAW, substituting however the somewhat higher residual element Linde 44 for the 44B. The heat analysis of the Hastelloy "X" and a weld pad analysis of the Linde 44 were used to predict compositions.

Shielded Metal Arc Welding

A similar approach can be taken to estimate the composition of deposited metal with either a tubular electrode with the second material at the center or for a solid core electrode with a ribbon attached along its length. In this case, however, the situations are more complex because the coating itself contains iron powder and must be considered as to increase the effective diameter of the electrode, figure 6,

$$\text{Effective Area} = \text{Core Area} \quad x \quad \frac{\text{Deposit Weight}}{\text{Core Wire Weight}}$$

where the weights involved are obtained experimentally. The expected concentration of each element is then calculated as follows:

$$C = \frac{(C_{Hx}) \, (A_{Hx}) + (C_c) \, (A_c)}{A_{Hx} + A_c}$$

where

      C = concentration of element in the deposited weld metal

      C_{Hx} = concentration of element in secondary wire of ribbon

      C_{Hx} = concentration of element in core wire or tube

      A_c = area of secondary wire or ribbon

      C_c = effective area of core wire or tube
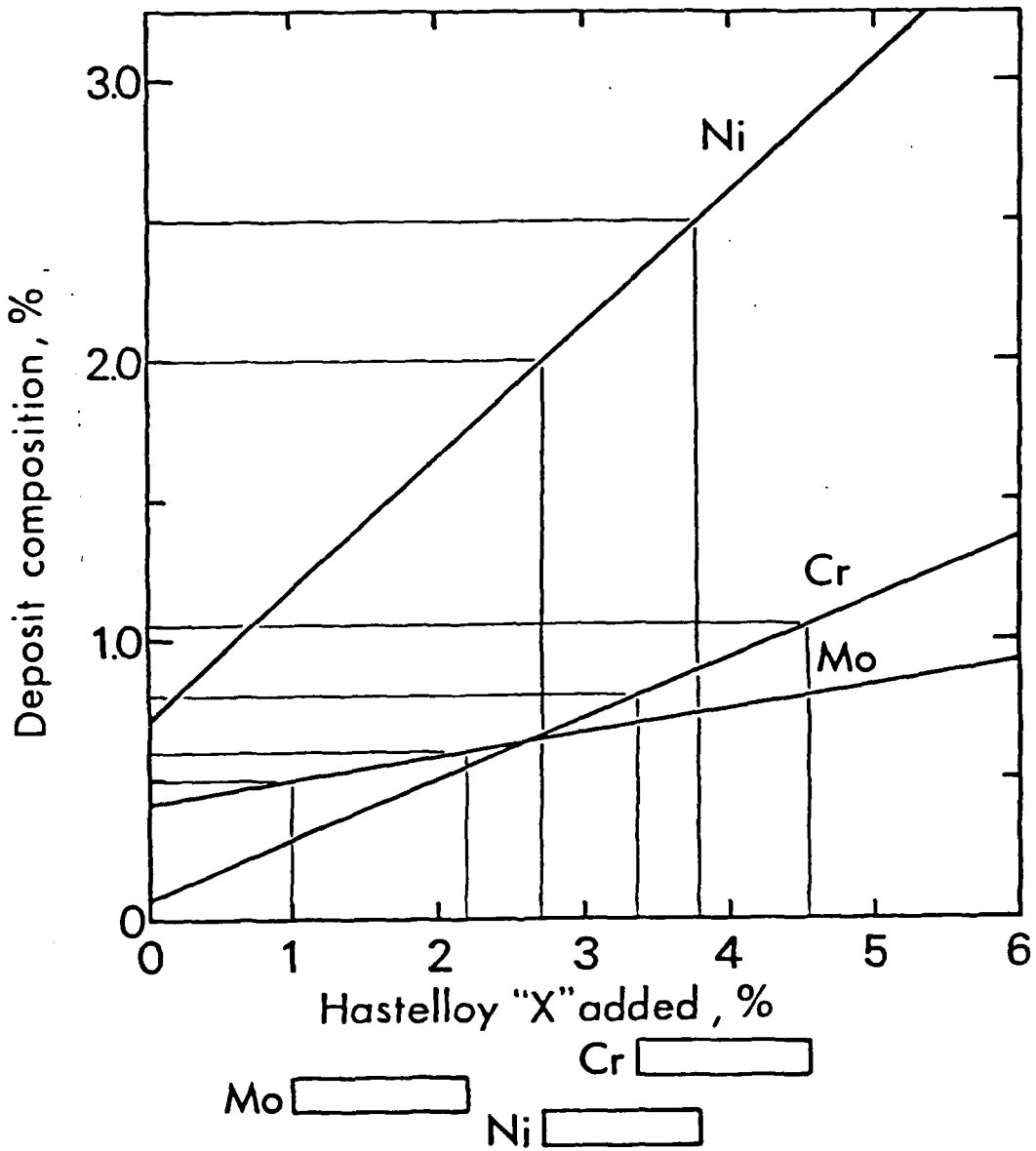
Figure 3. Plot of predicted deposit composition as a function
of secondary wire addition for Linde 44 and Hastelloy 'X'.
Bars below ordinate indicate AX140 composition limits.

13
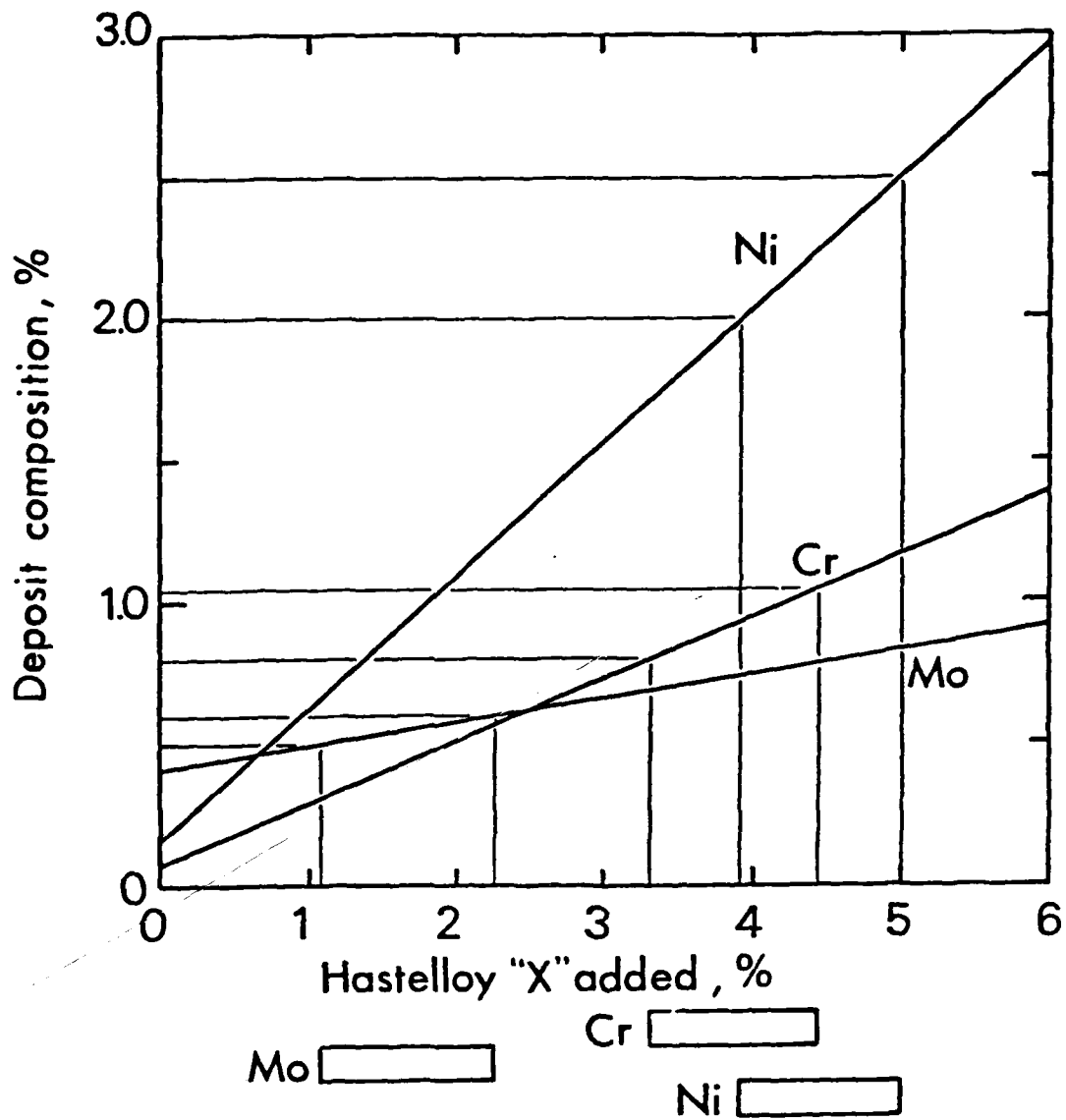
Figure 4. Plot of predicted deposit composition as a function of secondary wire addition for E80S-D2 and Hastelloy 'X'. Bars below ordinate indicate AX140 composition limits.

14
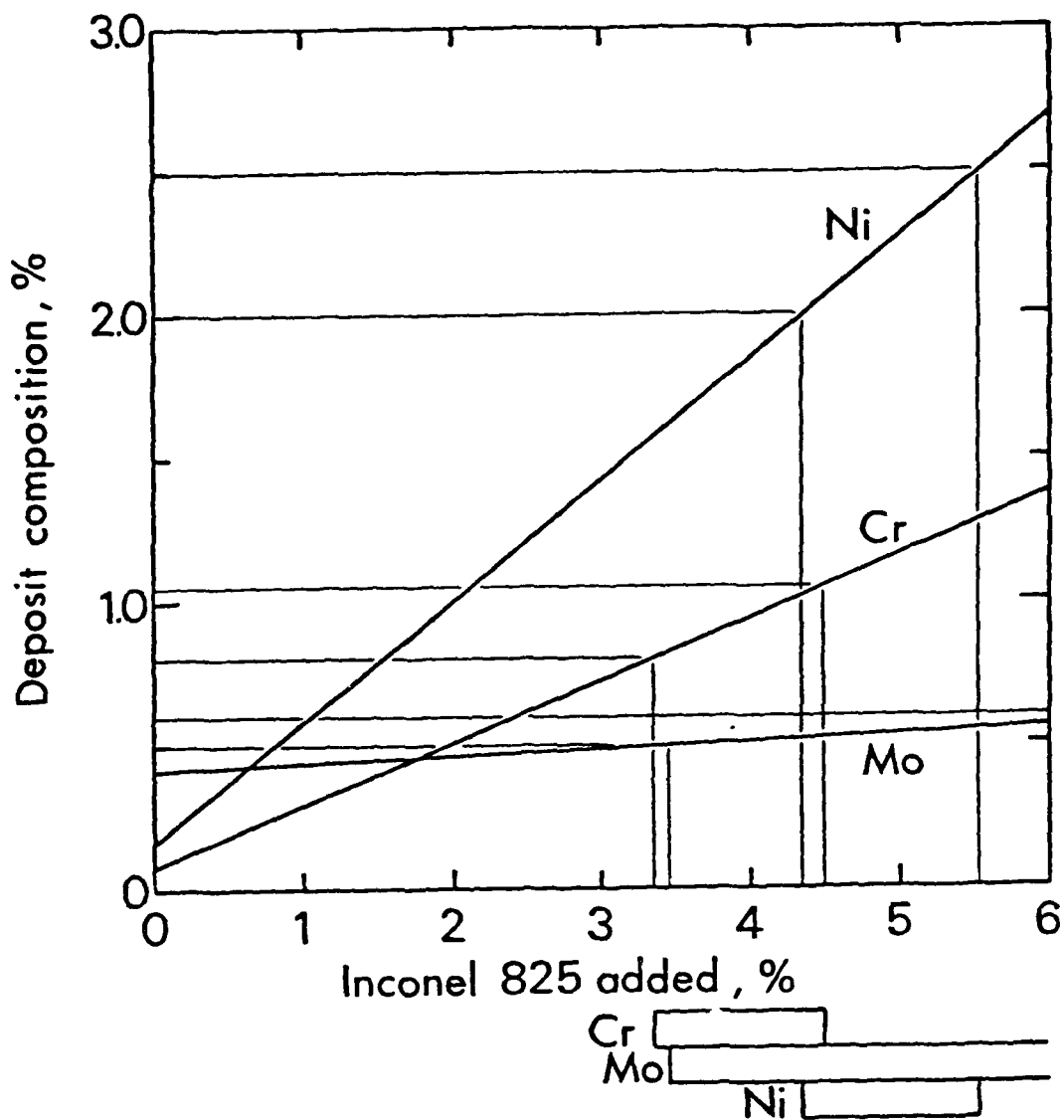
Figure 5. Plot of predicted deposit composition as a function of secondary wire addition for E80S-D2 and Inconel 825. Bars below ordinate indicate AX140 composition limits.
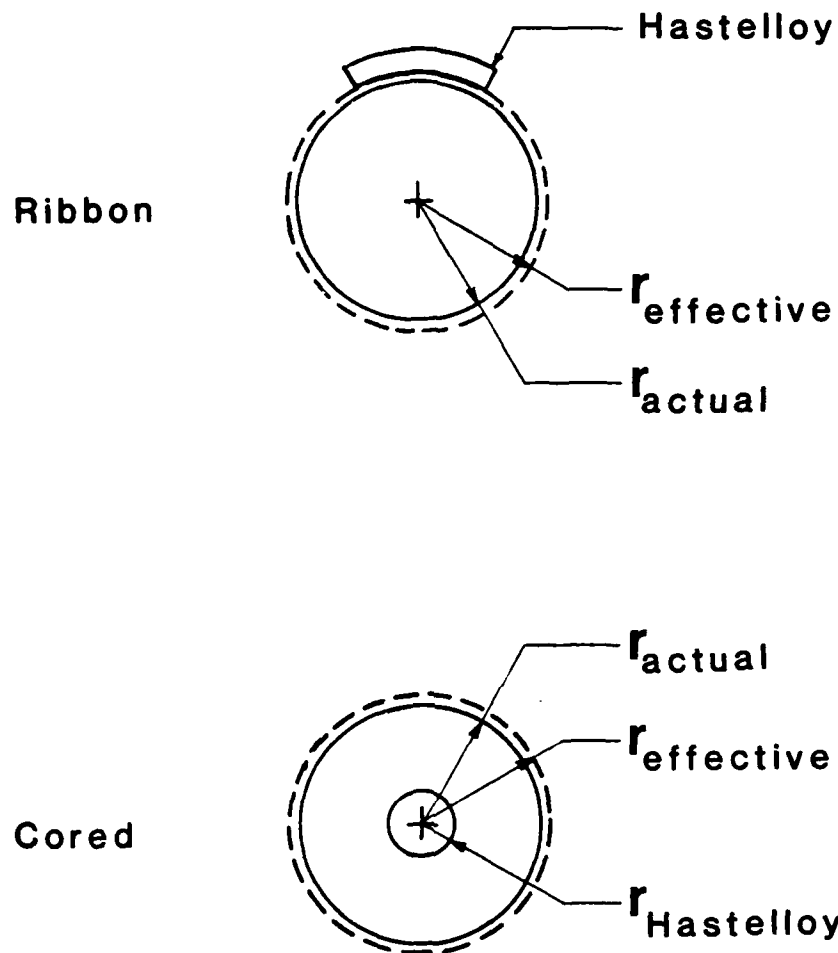
Figure 6. Composite electrode areas used to predict deposit chemistry. The Hastelloy area must be subtracted for the cored electrode. The effective radius accounts for iron present in the coating as pure powder and ferroalloys.

Transfer efficiencies of elements (e.g. Nickel, Chromium and Molybdenum) from the electrode to weld metal then be calculated according to the following equation:

$$E = \frac{C_{act}}{C_{exp}} \times 100 \tag{5}$$

where C_{exp} is the expected composition and C_{act} is the actual composition.

Manganese and silicon can be neglected in this analysis because they come mostly from the coating and are needed for electrode operating characteristics and deoxidation of the weld metal.

In attempting the new approaches to weld metal synthesis using two filler materials, several questions arose.

1) What commercial materials can be used to arrive at the target composition?

2) How can the two materials be fed effectively into the weld zone?

3) How good is the pool mixing at producing a homogeneous weld metal deposit?

4) How well do the mechanical properties of the weld metal compare to specification and those of conventionally produced weld metals?

These questions formulate the objectives of the present program.

The objectives:

To develop methods of synthesizing desired weld metal compositions in the SMAW, GMAW and SAW processes by introducing two filler metals into the weld pool simultaneously.

To investigate the adequacy of mixing of the components and relate homogeneity, microstructure and mechanical properties to specification and conventionally produced weld metals.

19

TECHNICAL APPROACH

This section of the report is arranged to describe the development of materials and equipment for each of the processes modifications SMAW, GMAW and SAW then the general experimental procedures common to all three are described. These include chemical analysis and methods for determining weld metal homogeneity, welding of the mechanical test plates and mechanical testing.

Shielded Metal Arc Welding

Preliminary investigation.

Two techniques were investigated for making alloy additions to the shielded metal arc welding system. These techniques, illustrated in Figure 7, utilize alloy additions either in the form of a high alloy strip tack welded to the side of a core wire, or a high alloy wire placed down the center of a hollow tube. For the preliminary studies, the starting materials, listed in Table 4, were readily available and not optimum. They were considered primarily for evaluation of each method with respect to manufacturing techniques, electrode performance, element transfer efficiencies and weld metal homogeneity.

Cored-electrode development

Metallographic examination of welds made with both types of electrode indicated that the homogeneity of the weld deposit was very uniform. The overall chemical compositions of the deposits (as shown in Table 5) was "lean" in carbon, nickel, manganese and molybdenum but "rich" in chromium, compared to the commercially available E14018. The compositions were so far removed that it was decided not to undertake a mechanical testing program.

Both electrodes operated in an optimum way during welding trials, as described later.

The thick-walled tubing that formed the bulk of the Hastelloy-cored electrode's core wire was swaged, reducing its inside diameter to just slightly larger than the Hastelloy wire diameter. It was then cleaned by flowing acetone through it, followed by acetone-soaked and then dry pipe cleaners, until the pipe cleaners came out with no evidence of contamination. The 0.035 in. (0.89 mm) Hastelloy 'X' wire was inserted and the combination drawn down to an OD of 0.156 in. (3.96 mm). The Hastelloy wire changed very little in diameter during this process.

Since the finished core wire for the cored electrode would be identical with an ordinary core wire in dimensions and outward appearance, no difficulty in the coating operation was expected. The drawing lubricant was cleaned from the outside surface with acetone, the composite was cut into 14 inch lengths, and prepared for coating by cleaning with emery cloth.

Ribbon Electrode Development

The Hastelloy "X" was the same used in the GMAW experiments (see Table 4). The 0.035 in. (0.89 mm) diameter wire was rolled to a thickness of 0.009 in. (0.23 mm), resulting in a ribbon about 0.095 in. (2.41 mm) wide, and cut to a length of 13.5 in. (34.2 cm). The work hardening and crookedness resulting from the rolling operation were found to impede subsequent operations, so the ribbon segments were annealed in flowing helium at 1800 F (982C) for 30 minutes. The surface contamination resulting from rolling and annealing was removed with emery cloth and the ribbons cleaned in acetone. 5/32 in. (3.96 mm) diameter electrode core wire was obtained and submitted for chem-

22
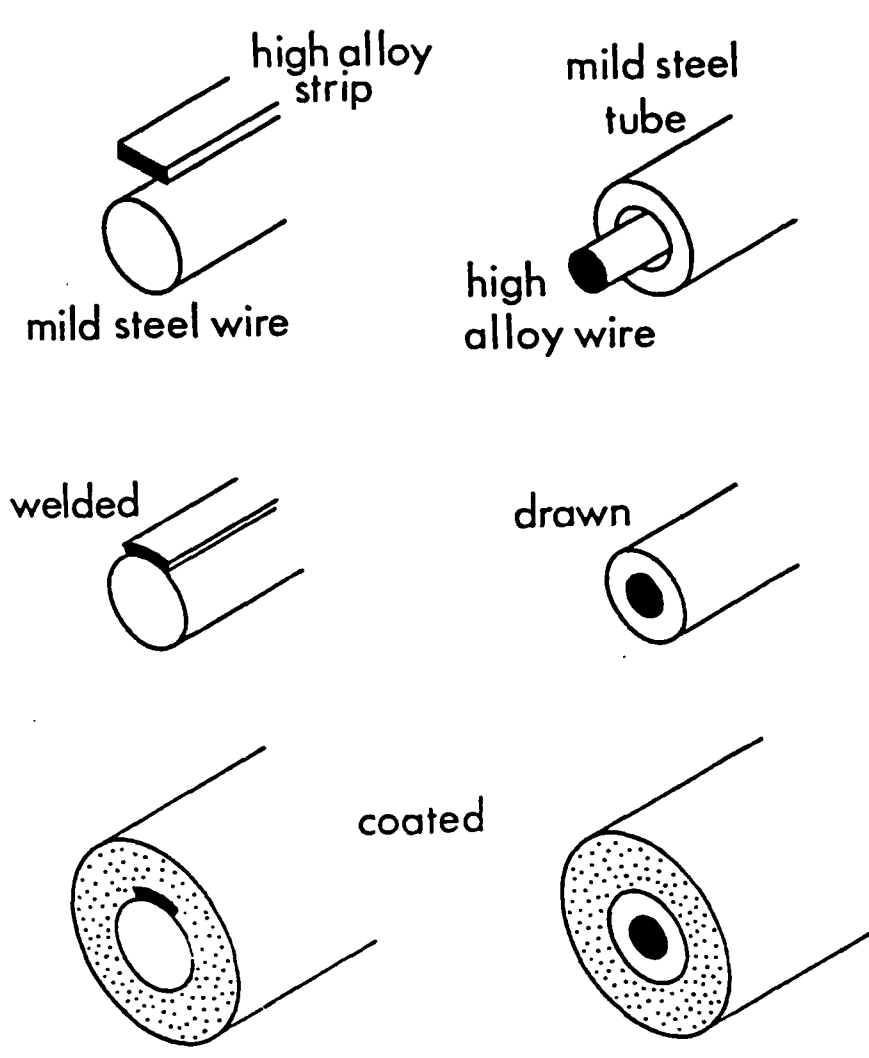
Figure 7. Schematic procedures for fabricating ribbon (right) and cored (left) composite electrodes.

TABLE 4.   STARTING MATERIAL COMPOSITIONS FOR SHIELDED
METAL-ARC WELDING -- DEVELOPMENT PHASE
(Weight Percent)

Element	Core Wire	Tube	Hastelloy X
C	0.037	0.073	0.07
Mn	0.53	0.41	0.60
Si	0.012	0.21	0.37
P	0.009	0.027	0.37
S	0.023	0.042	0.002
Ni	0.016	0.12	46.7
Cr	0.010	0.15	21.98
Mo	0.007	0.024	8.87
Co	0.003	0.012	1.93

Table 5.   Shielded Metal-Arc Deposit Compositions
During Development Phase
(Weight Percent)

Element	MI-30-CE/3 Specification Requirements	E14018 McKay Lot 1443690	Cored Composite (Hastelloy X)	Ribbon Composite (Hastelloy X)
C	0.10 max	0.054	0.041	0.038
Mn	0.75-1.35	0.98	1.08	0.86
Si	0.65 max	0.25	0.58	0.28
P	0.013 max	0.009	0.024	0.013
S	0.01 max	0.004	0.027	0.019
Ni	3.10-3.90	3.53	1.91	1.50
Cr	0.35-1.2	0.59	0.93	0.66
Mo	0.3-0.9	0.87	0.37	0.29
Co	---	0.016	0.10	0.076

ical analysis (see Table 4). It was also cleaned with emery cloth and acetone. The ribbons were carefully aligned with the core wires and spot welded at 70-90 watt-seconds with a Hughes Model VTW-30B resistance welder whose electrodes had been shaped to the desired outside contour of the ribbon. The welds were placed about 0.5 in. (12 mm) apart.

The electrodes were coated by Airco Welding Products Inc. using their standard type E7018 Moisture Resistant coating. This coating contains iron powder, ferro-manganese, and ferro-silicon but little or none of the Ni, Cr, and Mo powders of the standard E14018 coating. The coating operation proceeded quite smoothly, with a loss rate of less than 10% of the 120 electrodes coated, all of these from ribbon electrodes on which the spot welds failed and the ribbon popped off and either fouled the machine on feeding or cracked off the coating afterwards. Some of these defective electrodes proved to be operable for part of their length if the coating was not disturbed near the striking end. An unexpected beneficial effect of the coating operation was that the rollers feeding the electrodes through the pressurized coating mixture usually brought the ribbon into permanent close conformance with the core wire, although not consistently.

Figure 8 shows cross-sections of the composite electrodes, ground through 600 grit and unetched. Note that in Figure 8b the ribbon went through the drive rolls in such a way that it conformed to the core wire, while in Figure 8c it did not. Note, in all three cases, the relatively large size of the iron powder in the coating. Note also, in Figures 8b and 8c, the concentricity effects of the ribbon. The major dimension of the ovoid cross-sectional shape of the ribbon electrode's composite core is approximately centered in the extrusion die. The typical 0.004/0.005 in. (0.10/0.13 mm) concentricity requirement thus does not seem to be severely disturbed by the asymmetry of the core wire.

Manufacture of Electrodes for Weld Testing

The second phase of the development concentrated on fabrication of electrodes with the correct deposit composition, or close to that of the qualified electrode, for mechanical property evaluation. Since both the cored and the ribbon types of electrode yielded acceptable operating and mixing characteristics, it was decided to use the ribbon technique due to the simplicity and projected cost. The electrode size was changed from 5/32" to 1/8" and Hastelloy C-4 alloy was selected as the high alloy strip material based on element transfer efficiencies and the final deposit composition desired. The core was chosen to be a standard type of rod used for the manufacture of E-7018 electrodes.

Standard E-7018 electrodes contain iron powder in the coating. This results in an electrode deposition efficiency greater than 100% of the core wire weight. To calculate the size of Hastelloy strip necessary, this efficiency must be known. Trial welds were made to determine this efficiency by using 1/8", E-7018 electrodes with a coating similar to the type to be applied to the experimental electrodes. Weld deposits using these electrodes were produced on steel coupons of a known weight. The initial weight was then subtracted from the final weight to determine the amount of material deposited. The efficiency was then calculated using the following formula.

26
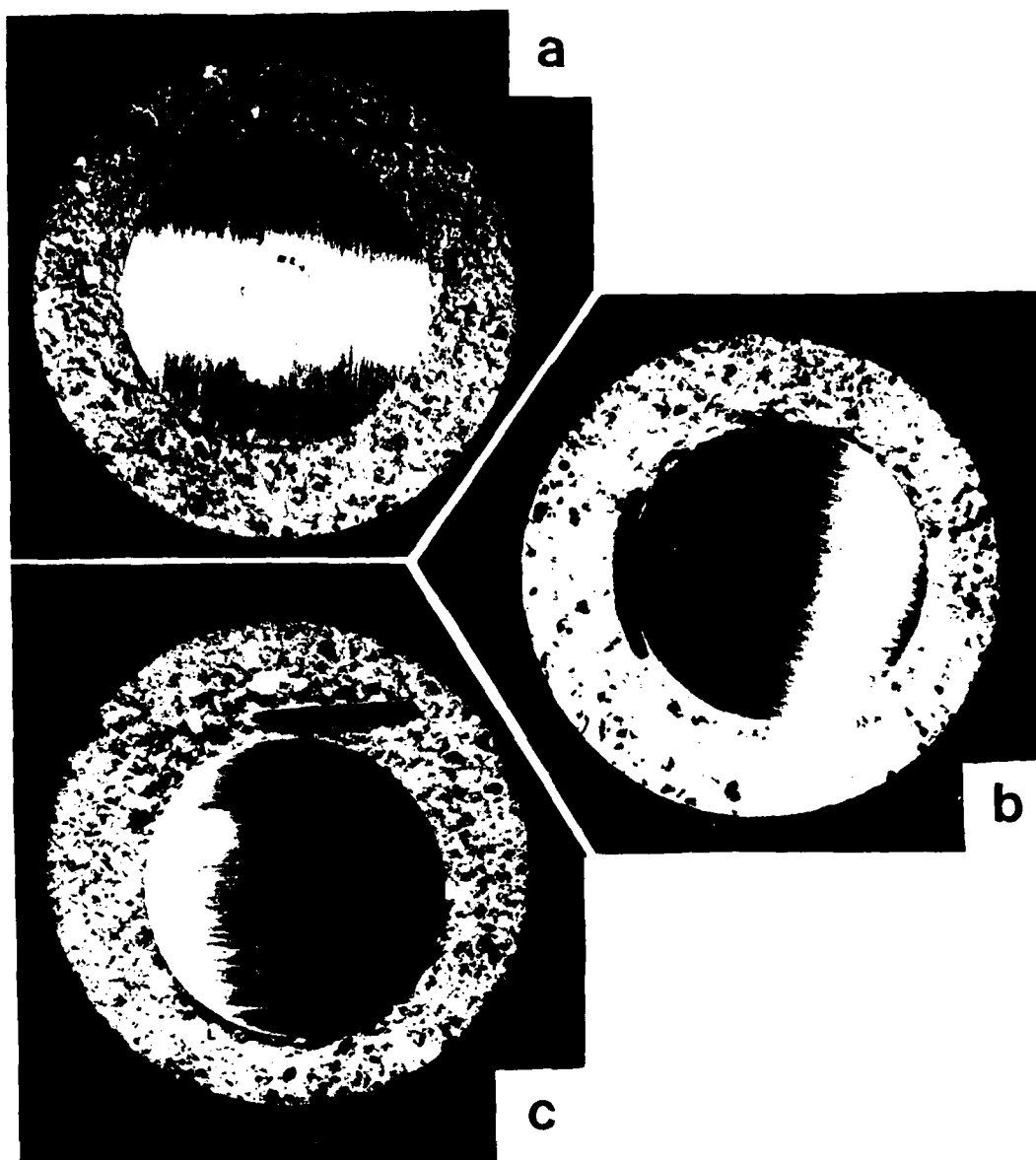
Figure 8. Cross sections of composite electrodes:
(a) cored electrode, Hastelloy 'X' core wire
(b) ribbon electrode in whch the ribbon conformed
    to the core wire
(c) ribbon electrode in which the ribbon did not
    conform to the core wire

(10X, unetched)

$$\text{Deposition efficiency} = \frac{\text{weight of deposited metal}}{\text{weight of core wire consumed}} \times 100$$

For this type of electrode under standard operating conditions, the deposit efficiency was determined to be 117%.

The composition of a typical E-14018 was selected as a target. This composition is close to the center of the range specified for MIL-14018-M1 electrodes. Two additional compositions, at the high and low end of the ranges were also selected. This was done to increase the chances of obtaining the desired composition. Table 6 shows the compositions of the starting materials and the calculated major alloying element content of the three fabricated ribbon electrodes.

Since the amount of ribbon required on the electrode was very small (approximately 4% by weight), it was necessary to produce strips to very tight dimensional tolerances. This was accomplished by precision rolling and slitting of the Hastelloy C-4 alloy according to the schedule below.

Production of Strips - 4 pieces of Hastelloy C-4 alloy sheet (4"x48"x1/16") were GTA welded end-to-end to produce a final strip 4" x 16' x 1/6"

    Rolled to about 0.03" thick
    Solution Anneal 1 hr. at 1950 F
    Rolled to about 0.015"
    Solution Anneal 1 hr. at 1950 F
    Rolled to 0.008" plus/minus .0004"
    Slit to widths of 0.096", 0.102", 0.112" plus/minus .001"

The cross sectional area of the ribbon was increased by about 10% to allow for estimated transfer efficiency of the alloying elements, and the width had to be altered slightly due to availability of slitting knife widths. This procedure resulted in about 100ft. coils of Hastelloy ribbon in three different widths, with extremely close tolerances. To provide enough material for all the mechanical property requirements, 500 electrodes of each composition were produced. The procedure for fabrication of the composite ribbon electrodes is listed below:

    Cut strips to 14" lengths
    Clean strips and core wire with methyl alcohol
    Tack the strips to the end of the core wire with three resistance welds
    Form the strips to conform to the surface of the core wire using grooved
                                electrodes on a seam welder (no power)
    Tack the strips every 1/2" using a capacitor discharge spot welder
    Straighten the core wires by hand

The core wire and ribbon were then coated by Airco Welding Products, Inc.

A standard moisture resistant E-7018 electrode coating was applied. One of the few problems encountered was with the clearance in the back die. The normal clearance for core wire in the back guide is about 0.003" (0.128" die for 0.125" electrode). Therefore, the 1/8" rod with ribbon attached would not fit and so a 5/32" back die was used. This situation led to some eccentricity of the core wire with respect to the eventual coating. The

28

TABLE 6. STARTING MATERIAL COMPOSITIONS AND CALCULATED DEPOSIT COMPOSITIONS FOR SHIELDED METAL-ARC WELDING--DEVELOPMENT PHASE

(WEIGHT PERCENT)

Element	Mil 14018-M1	Typical McKay 14018	1/8" DIA. Core Wire (SMAW)	Hastelloy C-4	Low Alloy .096" Width	Calculated* Med. Alloy .102" Width	High Alloy .112" Width
C	0.10 max	0.054	0.10	0.003			
Mn	.75-1.35	0.98	0.53	0.12			
P	.013 max	0.009	0.016	0.005			
S	0.10 max	0.004	0.025	0.002			
Si	0.65 max	0.25	0.009	0.02			
Ni	3.1-3.9	3.53	0.02	67.24	3.1	3.5	3.9
Cr	.35-1.20	0.59	0.015	15.90	0.68	0.79	0.88
Mo	.30-1.0	0.87	0.012	14.90	0.72	0.81	0.90

* Actual ribbons were slit slightly wider than calculated. This is due to availability of slitting knife widths and to compensate for element transfer efficiency.

29

coated electrodes were baked to cure the coating. During this treatment the electrodes bowed slightly, probably due to the differences in thermal expansion characteristics and strength levels of the core wire and the strip.

The following electrodes were produced:

> 500 each with 0.096" strip
> 500 each with 0.102" strip
> 500 each with 0.112" strip
> 100 each with no strip - (control group)

After coating was completed, pads were welded for determination of deposit composition. Based on these results, shown in table 7, the 0.096" electrodes were selected for welding of the test plates.

The specification requires 1/8" diameter electrodes to be qualified in the vertical welding position. During welding of the first plate surface porosity was observed in some passes and it was then decided to weld the final plate in the flat position. A subsequent radiographic examination revealed large amounts of porosity in the vertical position weld and much smaller amounts in the flat position weld. It was therefore decided to take tensile samples taken from the vertical weld in areas selected to minimize porosity in the gage section. Dynamic tear samples were machined from the flat weld. Results of electrode operability and mechanical properties are given in the results section of this report.

TABLE 7. SHIELDED METAL-ARC DEPOSIT COMPOSITIONS-PRODUCTION PHASE ACTUAL DEPOSITS

(WEIGHT PERCENT)

Element	Mil 14018-M1	Typical McKay 14018	Low Alloy .096" Width	Med. Alloy .102" Width	High Alloy .112" Width
C	0.10 max	0.054	0.04	0.04	0.04
Mn	.75-1.35	0.98	0.74	0.74	0.74
P	0.13 max	0.009	0.016	0.017	0.015
S	.010 max	0.004	0.019	0.021	0.017
Si	0.65 max	0.25	0.63	0.65	0.63
Ni	3.1-3.9	3.53	3.51	3.78	4.21
Cr	.35-1.2	0.59	0.77	0.82	1.03
Mo	.30-1.10	0.87	0.79	0.86	0.88

31

GAS METAL ARC WELDING

The development of the gas metal arc welding system, which employed the simultaneous feeding of two wires in the weld zone, took place in three phases.

(1) "Cold"[*] wire feeding of the second wire into the pool
(2) "Cold" wire feeding of the second wire at the top of the arc
(3) Dual "hot" wire feeding.

Figure 9 shows schematically the three methods of feeding the second wire.

Material Selection

Based on all considerations, it was decided that a combination of an E80S-D2 (main wire) and Hastelloy X would produce a composition of weld metal closest to the composition of the Linde L-140 (a previously qualified wire). Table 8 provides the compositions of the various wires selected together with those of specified composition ranges and the qualified wire.

Equipment

The equipment used here for welding with secondary wire feed included the following:

   Hobart Mega-MIG 650 RVS constant potential power supply with Mega-Con 110 controller

   Hobart 371046-3 wire feeder for primary wire, controlled by Mega-Con 110

   Arc Systems controller and side beam

   Linde 7110-270 wire feeder for secondary wire, controlled by Arc Systems controller

   Hobart 600-amp water-cooled GMAW torch (Method 1 and 2)

   Linde ST-12 (Method 3)

   Jetline digital wire feed meters

Power supply and electrical hookups were according to standard policies, except that specimens were insulated and grounding was kept mobile (rather than random through table contact) to investigate and control ground current flow effects on pool stirring.

[*] "Cold" and "Hot" refer to whether the second wire was part of the elctrical circuit.

MAIN
WIRE

section a-a
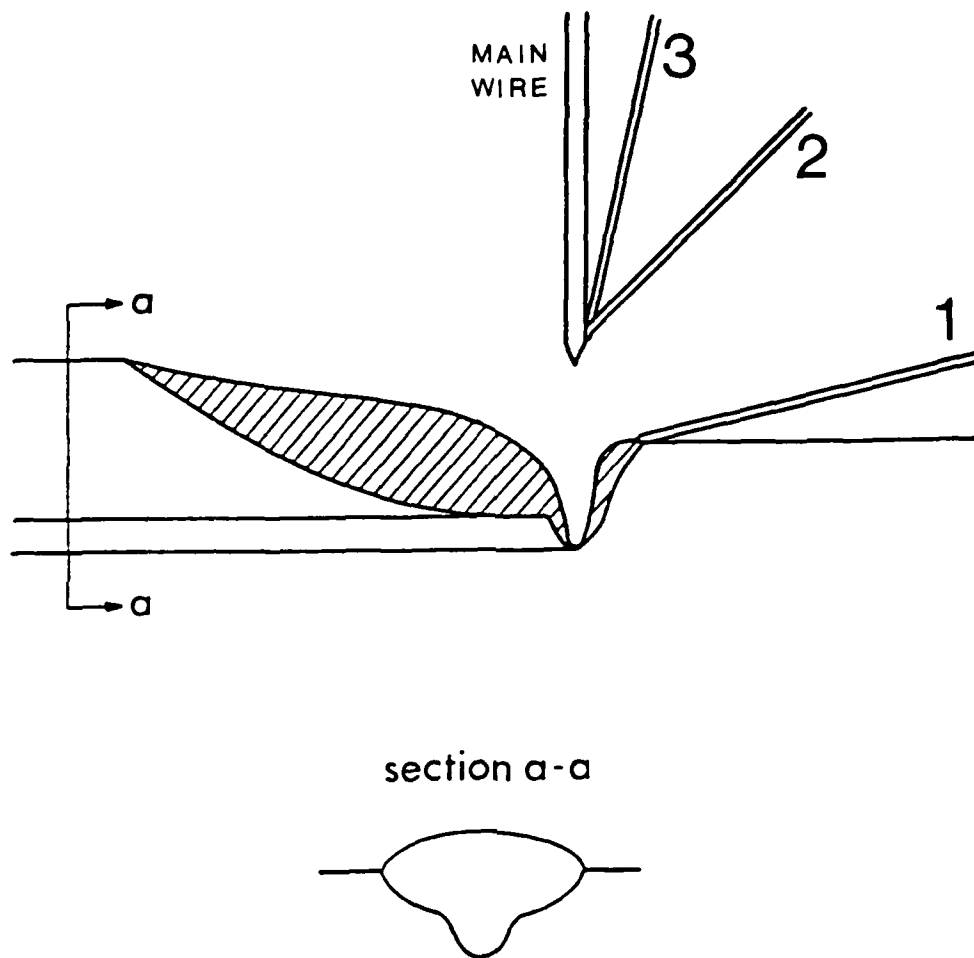
Figure 9. Schematic illustration of Gas Metal Arc secondary
wire addition methods.

Method 1: cold wire feed at pool leading edge

Method 2: cold wire feed above arc

Method 3: dual hot wire

33

TABLE 8.   STARTING MATERIAL COMPOSITION FOR GAS METAL ARC WELDING

(Weight Percent)

Element	Specification Mil 140S-1	L-140	Hastelloy X	HR 18* Old Heat #D 7024	HR 18** New Heat #F 1856
C	.012 max	.06-.12	.07	.08	.08
Mn	1.5-2.0	1.5-1.9	.53	2.09	1.81
P	.01 max	.01 max	.014	.014	.014
S	.01 max	.01 max	.002	.025	.019
Si	.3-.5	.35-.45	.37	.69	.64
Ni	1.95-3.1	2.3-2.9	46.7	.060	.057
Cr	.65-1.05	.65-.90	21.58	.073	.053
Mo	.4-1.0	.7-1.0	8.87	.50	.50
Co	-----	-----	1.93	-----	-----

*   Used for GMA 01

** Used for GMA 02-GMA 04

34

Method 1. Cold wire feeding of the second wire into the pool.

The experimental set-up for feeding the second wire is shown in Figure 10. The secondary wire and wire feed system were insulated from the rest of the welding system to avoid possible welding current flow.

Wire feeding procedures were developed by trial and error to obtain smooth feeding of the secondary wire into the puddle, subject to several constraints: (1) the wire had to feed fast enough to avoid "balling up" due to arc heating and consequent intermittent alloy addition, but slowly enough to melt shortly after entering the puddle; (2) shape and positioning of the secondary wire guide tube had to permit the use of standard joint designs; (3) mixing due to turbulent flow in the weld pool had to be sufficient to homogenize the deposit.

"Balling up" and passing through the puddle unmelted are two extreme results of inappropriate secondary wire size or composition. Therefore, choice of secondary wire composition is related to wire size and feed rate mainly by iron content: the iron dilutes the alloying elements and increases the required feed rate. A wire that must be fed too slowly (i.e., is too rich in alloying elements or too large) leads to balling-up, while a wire that must be fed too fast can pass through the weld pool without melting. Test welds were made to optimize the uniformity of the secondary wire feed, resulting in the parameters listed below

Current	350 A
Voltage	28 V
Travel Speed	13 ipm
Primary wfs	200 ipm
Secondary wfs	2040 ipm
Shielding Gas	Ar2% Oxygen at a flow rate of 50 cfh

Smooth secondary wire feeding was achieved by adding the secondary wire at a shallow angle at the front edge of the puddle, much as in standard practice for GTAW, as in Figure 9. The secondary wire guide tube could easily extend into the joint, and the deeply penetrating spray arc passing directly over the wire addition would presumably produce good mixing.

This method was eventually discarded because of pool mixing problems, to be discussed later. It was deemed necessary to feed the second wire into the top of the arc to improve homogeneity.

Method 2. Cold wire feeding of the second wire at the top of the arc.

In order to feed the wire into the top of the arc a special torch nozzle had to be designed and is illustrated in Figures 11 and 12.

The technique consisted of feeding an electrically insulated secondary wire onto the main wire at a point just above the arc. With the wire at the optimum position feeding was smooth and complete mix. in the weld metal was achieved as shown in Figure 13. The secondary wire was observed to melt by arc heating and flow onto the surface of the main wire under surface tension forces and the combined molten metals were transferred across the arc.
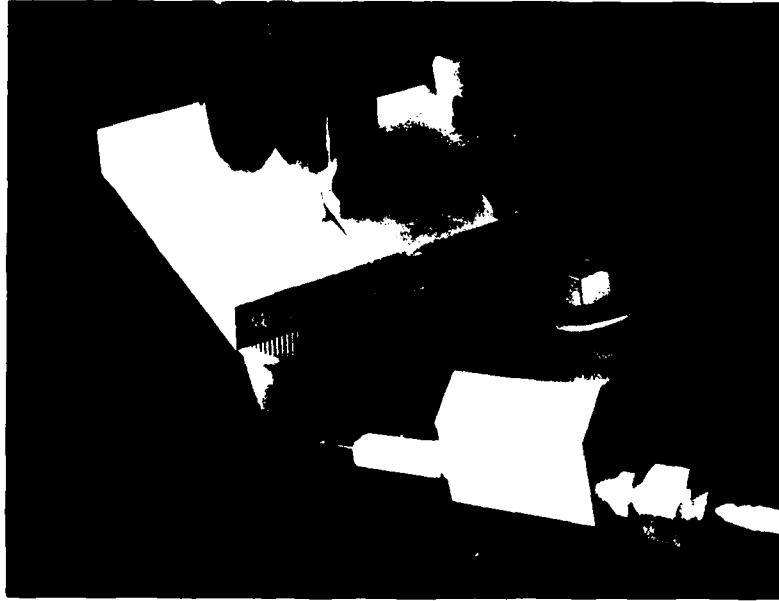
Figure 10. Apparatus for cold wire feed into Gas Metal Arc
weld pool.
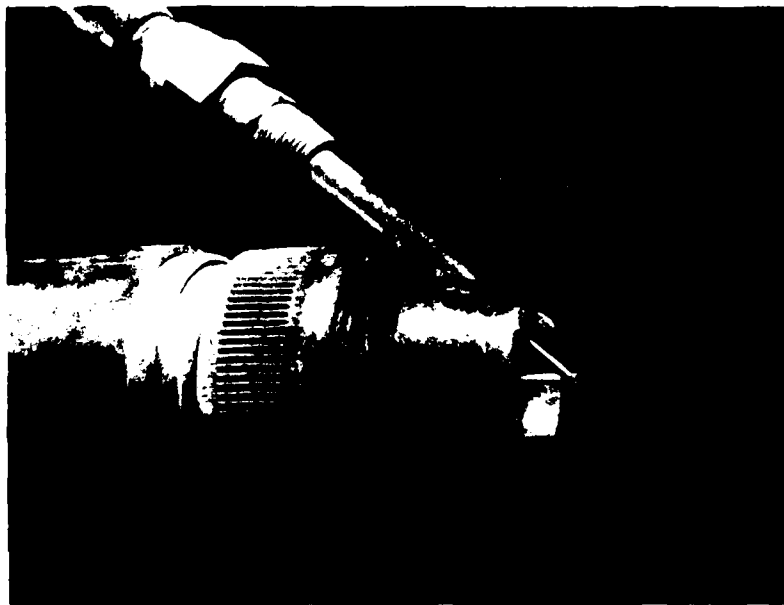
Figure 11. Apparatus for cold wire feed above arc.
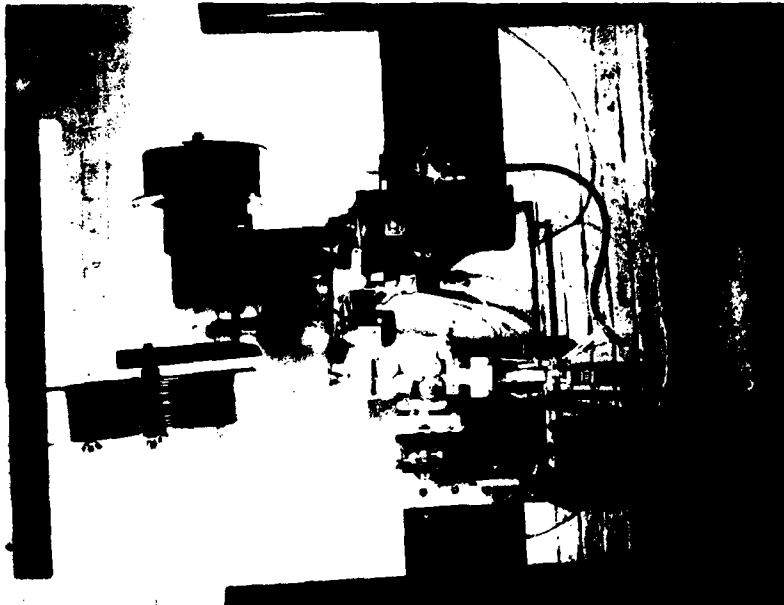
Figure 12. Side beam carriage equipped for feeding two wires.

37

Figure 13. Metallographic cross sections of a weld pro-
duced with the torch at optimum height. Note uniformity
in the fusion zone.

   Section (a) transverse to plate surface, along weld
            centerline

   Section (b) parallel to the top plate surface

The main problem with this technique was sensitivity to torch height. If torch to work distance was decreased, the secondary wire would tend to feed into the arc, ball up and drop off only when the mass of the ball overcame the surface tension. This resulted in lack of uniformity in the weld deposit (Figure 14). With a torch to work distance greater than optimum the secondary wire tended to feed past the main wire a short distance. It then started to ball up, then flow back onto main wire as before, although somewhat randomly. Again, this process led to inhomogeneities of the weld metal as shown in Figure 15, although not so pronounced as when the torch to work distance was too short.

This sensitivity to arc length and torch to work distance rendered the system unsuitable for practical welding.

Method 3. Dual hot wire feeding.

Decreasing the angle between the secondary and main wire would decrease the sensitivity to height variations (Fig. 9). The most practical way this could be accomplished was by feeding the wires through a contact tube assembly modified to accommodate both wires, although now the secondary wire could no longer be insulated. A prototype assembly consisting of two contact tubes and a modified gas cap was fabricated for the existing torch and tested. This resulted in much more tolerance in height variations, although it was not reliable due to binding of the second wire in the curved contact tube. Based on the performance of this first prototype, it became necessary to modify a standard GMA torch to accommodate the second wire and provide reliable feeding. The design of a Linde ST-12 torch was the most conducive to modification. The torch was modified as shown in Figures 16 through 19. This torch proved to feed the wire more reliably and also provided better gas coverage than the previous torch, as judged by weld surface appearance and the occurrence of porosity at large torch-to-work distance. The new torch design was evaluated for mixing characteristics using a technique shown schematically in Figure 20. In this experiment the arc was initiated with a contact tube to work distance (CTWD) of 1/2". As welding progressed, the torch to work distance was effectively increased by the sloped plane. The weld was terminated with a 1 1/4" CTWD. This change in CTWD is much greater than would normally be encountered.

To evaluate this change on the macroscopic homogeneity of the weld, the weld reinforcement was removed and the surface parallel to the plate surface was polished, etched and examined. Adequate mixing was observed along the length of the weld. This was confirmed later by spectrographic analysis of the weld metal at a series of locations. Very little scatter in the element concentrations was noted.

Feeding of the wire to the top of the arc, as opposed to feeding into the pool, did result in a greater loss of alloying elements from the secondary wire either by vaporization or oxidation. It was therefore necessary to adjust the secondary wire feed rate to compensate.

39
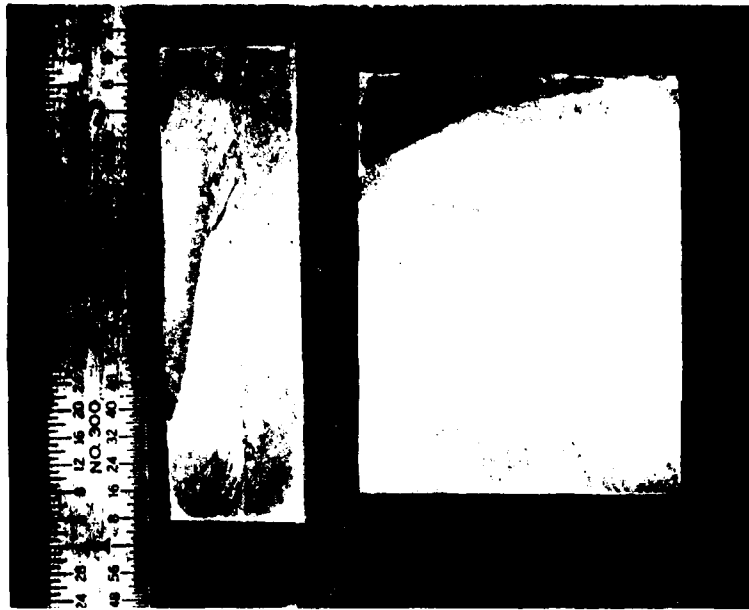
Figure 14. Metallographic sections similar to those in
figure 13, produced with torch 1/8" lower than optimum.
Note nonuniform mixing.
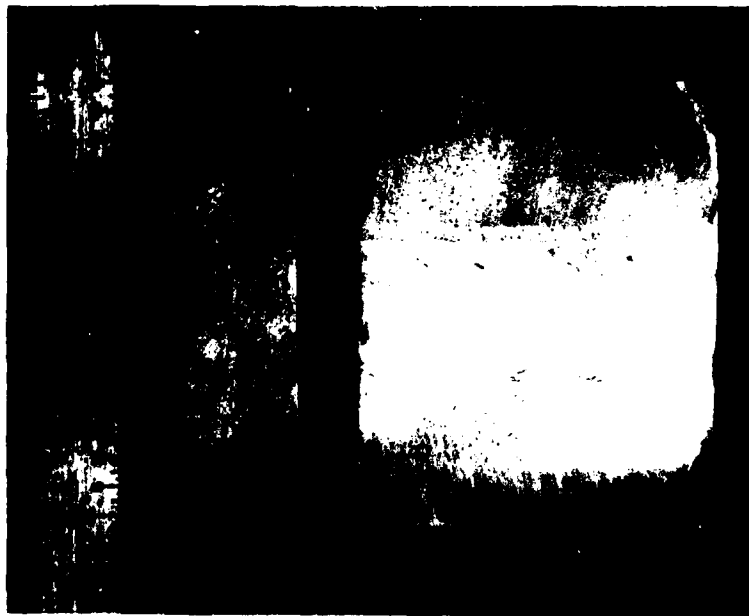
Figure 15. Metallographic sections similar to those in
figure 13, produced with torch 1/8" higher than opti-
mum. Note nonuniform mixing.
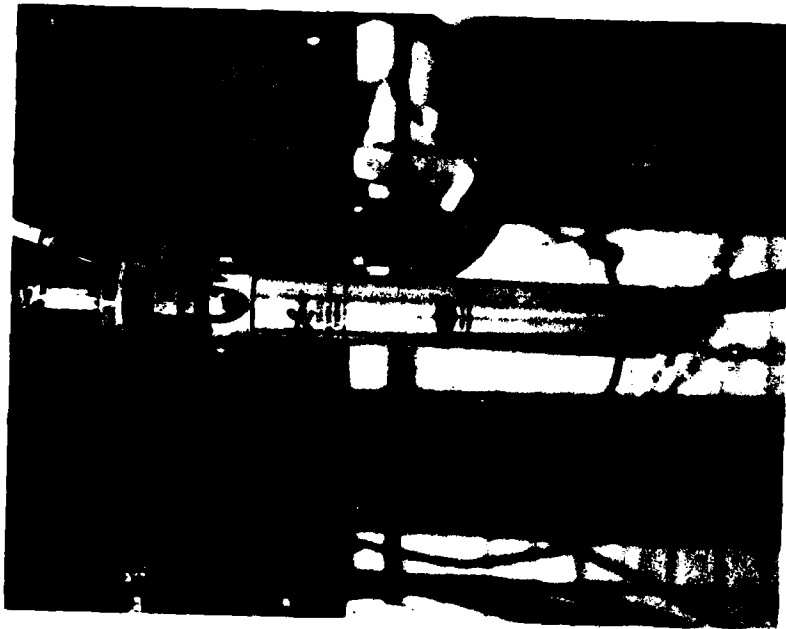
Figure 16. Final torch configuration for Gas Metal Arc dual hot wire method.

Figure 17. Torch modified for dual hot wire method, with outer barrel removed to show secondary wire route.

Figure 19. Side beam carriage equipped for dual hot wire method.

Figure 18. Contact tube and gas cup configuration for dual hot wire method.

42
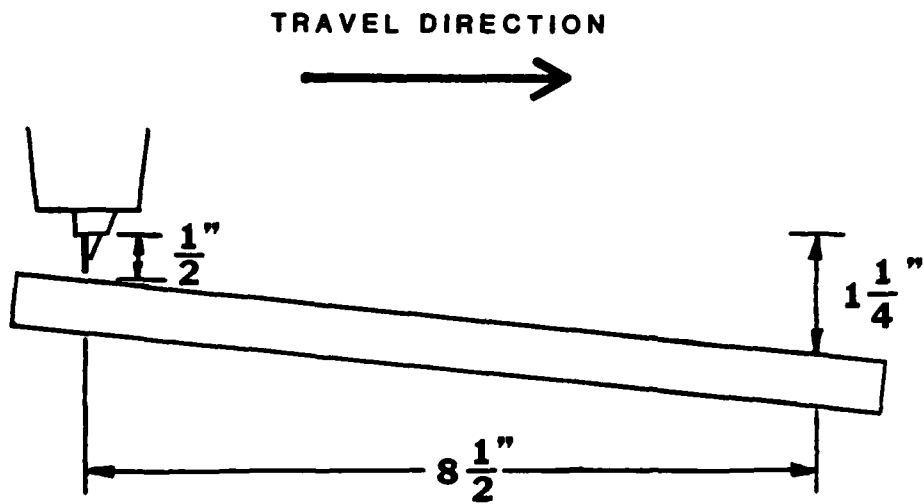
Figure 20. Schematic illustration of experiment to examine the effect of torch to work distance on Gas Metal Arc weld pool mixing.

GMA Welding Conditions

Initial attempts to make groove welds with method 2 torch resulted in some unanticipated problems. Severe porosity was encountered in the root passes whereas the same welding conditions and consumables used for making bead on plate deposits produced sound weld metal. Apparently, there was an adverse effect of shielding gas flow characteristics in the groove. Switching to the ST-12 torch with no other changed resulted in smoother operation in the groove, presumably because of the improved design and less intrinsic turbulence in gas flow. The first groove weld, GMA01, was welded with the following conditions:

Current	400 A
Voltage	28.5 V
Travel speed	19.2 ipm
Primary wfs	213 ipm
Secondary wfs	33 ipm
Contact Tube to Work Distance (CTWD)	5/8 inch
Shielding gas	Ar-2% Oxygen at a flow rate of 50 cfh.

Except for some solidification cracking and non-wetting in the root passes (which were ground out and rewelded), the welding went smoothly. Twelve hours later a small indication was noted on the weld surface. This was checked by magnetic particle inspection, and was found to be a transverse crack about 1/4" long. After 48 hours had elapsed after welding (as required by spec.), the backup strip was removed by carbon-arc gouging and ground flush. During radiographic testing the 1/4" indication on the surface was found to extend the full width of the fusion zone, and from the image density difference appeared to be fairly deep (Figure 21). Many other cracks not open to the surface, plus porosity, well in excess of the maximum allowable, were also detected. Ultrasonic inspection using a 6 dB drop technique and a straight beam transducer (through the end of the plate and parallel to weld axis) confirmed that the crack covered an area almost as large as the original groove area. A bend sample (3T) was taken from the end of the plate and broke through the weld during testing. In spite of this, it was decided to perform tensile tests, with the samples taken from areas between the large cracks. These samples exhibited very poor ductility (Figure 22) and a higher than desired yield strength.

The fracture surface was examined using scanning electron microscopy and it was confirmed that porosity was present in the fracture and that the specimen had suffered hydrogen damage. Figure 23 shows part of the fracture surface which illustrates the crack origin and a surrounding zone of cleavage fracture (see Figure 24). Outside of this zone, the fracture surface was ductile as shown by the dimpled fracture in Figure 25.

At this point, extensive effort was expended, to isolate the cause of, and elimination of the gas contamination which was thought to be responsible for both the porosity and the hydrogen damage. Shortly after welding the first plate an oily buildup was noticed on the serrated drive rolls for the main wire. This was a likely source of contamination for both porosity and hydrogen, but even after rolls were cleaned the porosity continued. All the porosity determination studies were conducted with bead on plate welds using the parameters listed previously for GMA01. Many different tests were
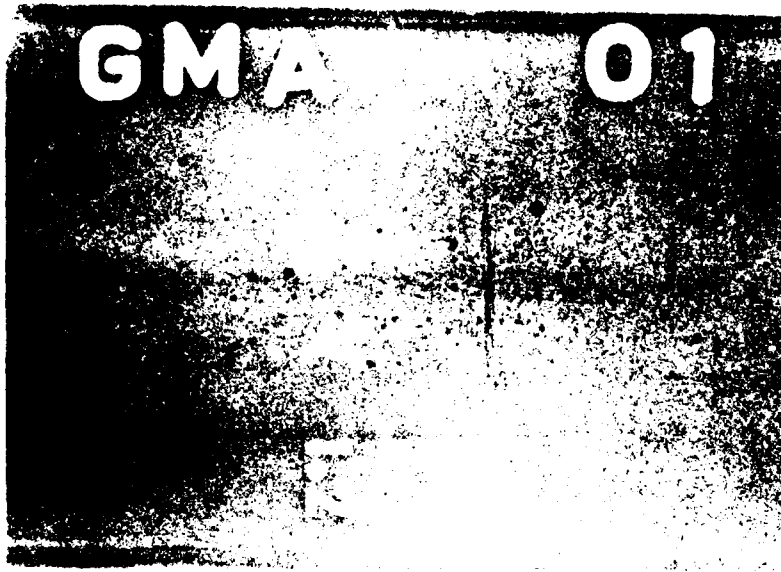
Figure 21. Portion of a xeroradiograph showing hydrogen in-
duced cracking and porosity in a Gas Metal Arc weld (GMA-01)
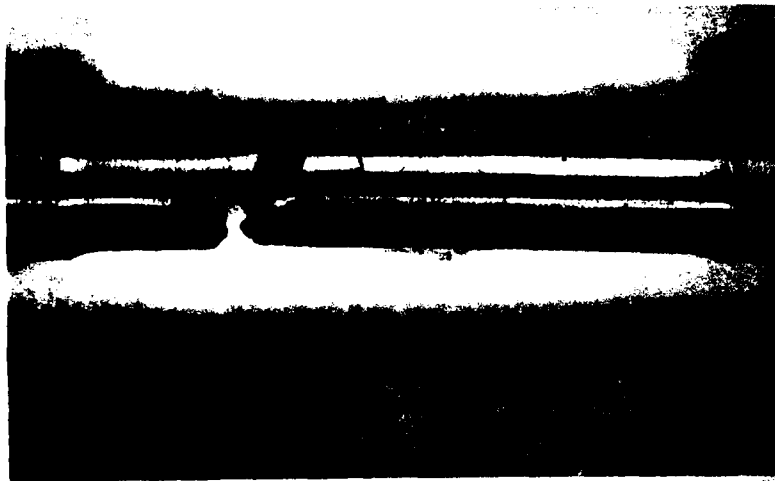
Figure 22. Tensile sample from GMA-01. note lack of ductility, irregular fracture, secondary cracking, and porosity.
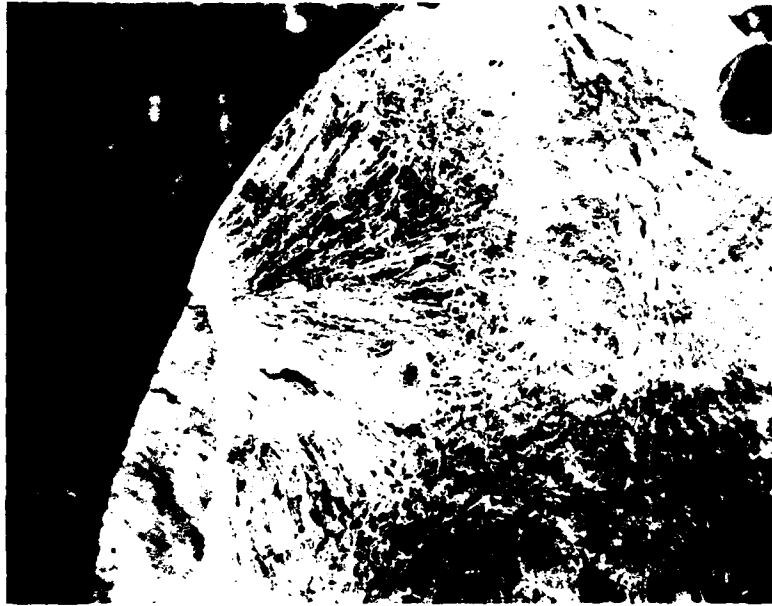
Figure 23. Fracture surface of GMA-01 showing regions of brittle fracture, ductile fracture, and porosity. (22X)
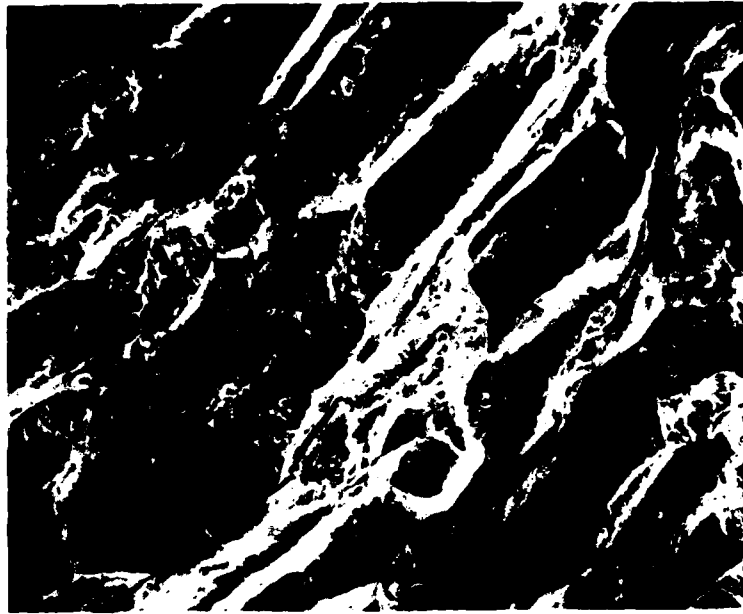
Figure 24. Zone of cleavage fracture suggesting hydrogen damage. (540X)
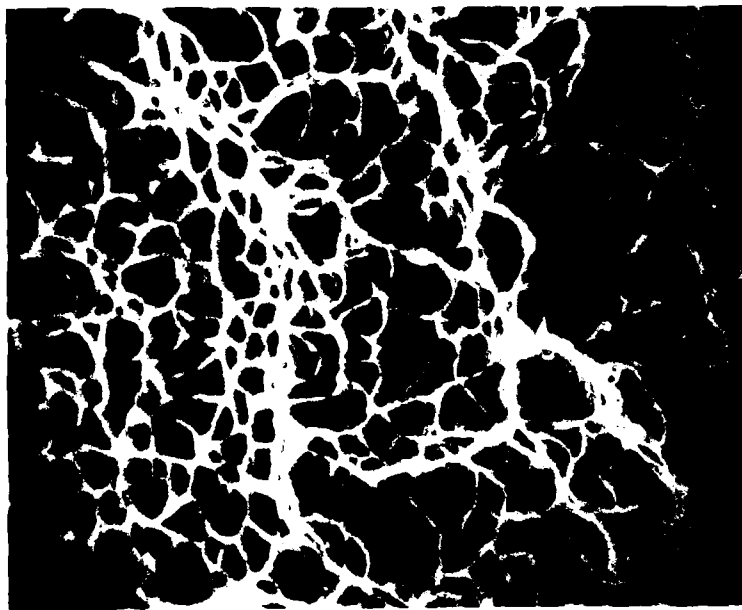
Figure 25. Ductile fracture zone. (2200X)

conducted, including varying torch height, cleaning the system, investigating condensation in torch barrel, etc. Although there were some inconsistencies, most of the factors indicated the secondary wire as the contamination source. This was somewhat puzzling because the same secondary wire was used independently for the submerged arc welds with no problems. The oxygen content of the wire was 0.051%, and, considering the small percentage of secondary wire used, this did not seem to be a likely source. The porosity was finally reduced to acceptable levels (although not eliminated) by altering the welding conditions. The current was kept as low as possible while maintaining a stable spray transfer, and the voltage was also lowered as far as possible without losing the acceptable bead contour. The travel speed was then lowered to get the heat input back into the specified range. The reduction in porosity was thought to result from lower solidification rates and a greater amount of time for the gas to evolve without becoming entrapped. Due to the overmatching of yield strength in the previous plate, the secondary wire addition was lowered to slightly decrease the alloy content. A second weld plate (GMA-02) was produced with the following modified conditions.

Current	320 A
Voltage	25.5 V
Travel speed	11 ipm
Primary wfs	176 ipm
Secondary wfs	25-26 ipm
CTWD	5/8 inch
Shielding gas	Ar-2% Oxygen at a flow rate of 50 cfh.

The anticipated weld metal composition, obtained from bead on plate pad tests was:

Carbon	0.05	%
Manganese	1.56	%
Phosphorus	0.013	%
Silicon	0.57	%
Nickel	2.11	%
Chromium	1.05	%
Molybdenum	0.87	%

No cracking was noted and the porosity had been reduced dramatically from the previous weld. A bend sample taken from the end of the plate was acceptable indicating good ductility of the weld metal, and the remainder of the plate was prepared for tensile testing. These samples yielded satisfactory results (GMA-02).

To produce the dynamic tear plate the heat input had to be reduced as is required by specification. Since the current and voltage were already at minimum levels (for this size wire) this could only be accomplished by an increase in the travel speed to 14 IPM (with all other conditions constant). Due to the lower deposition per pass and greater cooling time (mandatory lower preheat and interpass temperature), the plate could not be completed in one day. The plate was allowed to cool overnight in still air, as specified by thequalification procedure. The following morning several transverse cracks were observed. Radiographic inspection indicated that these cracks were similar to those encountered in GMA-01. In addition to this, the amount of porosity had increased, probably due to the increase in

travel speed. In order to obtain a weld plate for testing it was decided to weld the plate using the conditions listed for GMA-02 and to bake out the plate after welding (using the bakeout conditions established for SMAW: 12 hours @ 350F). This final plate (GMAW 04) contained no observable cracks, and a small amount of porosity. Dynamic tear samples were machined from this plate.

SUBMERGED ARC WELDING

Materials

There is at present no qualified system for the SAW welding of HY 130 mate
rial. In the absence of a weld metal compositional guideline it was decided
to use, as a target, a weld metal composition which has been successful for
GMAW, namely, the AX-140 wire composition. Linde 44, a submerged arc
welding wire and Hastelloy X as a secondary wire, were selected. The
appropriate compositions are given in Table 9, together with a predicted
weld metal composition.

Equipment

Essentially the same equipment used for the GMAW work was employed. There
was, of course, no need for gas shielding which was replaced by a suitable
flux. This flux was fed around the main wire.

Initial investigations were conducted using the secondary cold wire addition
technique (Method 1, figure 9). With the wire passing through granular flux
before reaching the arc, it was assumed that radiation heating from the arc
and balling-up of the second wire would not be as great a factor as in GMAW.
Direct observation and confirmation of this, however, was not possible due
to the layer of flux covering the arc and weld pool. Welds produced with
secondary cold wire feed were polished and etched for examination. Some
lack of mixing was noted, although the severity was not as extensive as that
observed in GMA welds produced in a similar manner. Switching to a dual hot
wire technique (Method 3, Figure 9; Figure 26) resulted in greater uniformi-
ty in the deposit.

Welding Conditions

Conditions were selected to remain within the heat input, preheat and
interpass temperature ranges established for GMAW, while producing good
operating characteristics and bead profile.

In establishing conditions to achieve the desired weld metal composition via
the bead-on-plate technique, some interesting observations were made in that
the composition was different than predicted. When using the Oerlikon
OP121TT flux and the following welding conditions

Current	330 A
Voltage	23.8 V
Travel speed	14 ipm
Primary wire feed	158 ipm
Secondary wire feed	18 ipm
CTWD	1/2 in.
Heat Input	33.7 kj/in.

there was a pronounced reduction in carbon and manganese, but an increase in
the silicon level of the deposit, compared to the predicted value (Table 10).
Wire compositions were rechecked and the experiment was repeated using a

51

TABLE 9. STARTING MATERIALS COMPOSITION FOR SUBMERGED ARC WELDING

Element	Mil 140S-1	AX-140	Linde 44 (SAW)	Hastelloy X	Calculated Deposit Composition
C	.12 max	.05-.09	.11	.07	.11
Mn	1.5-2.0	1.9-2.2	2.13	.53	2.07
P	.01 max	.01 max	.008	.014	.008
S	.01 max	.01 max	.008	.002	.008
Si	.3-.5	.25-.45	.083	.37	.09
Ni	1.95-3.10	2.0-2.5	.62	46.7	2.25
Cr	.65-1.05	1.0-1.25	.09	21.58	.84
Mo	.4-1.0	.5-.6	.41	8.87	.71
Co	-----	-----	-----	1.93	.07
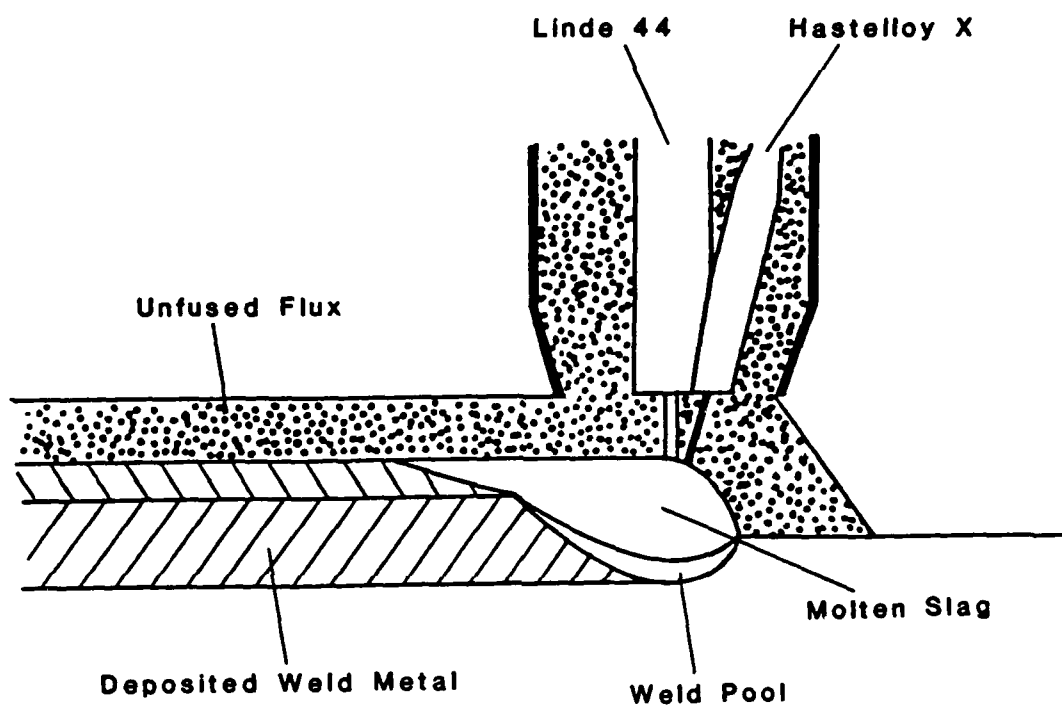
Figure 26. Schematic of dual wire Submerged Arc.

53

TABLE 10.   CHEMICAL COMPOSITION OF SAW WELD METALS OBTAINED USING TWO
            DIFFERENT FLUXES

Composition (weight percent)

Element	Predicted	OP121TT	880	OP121TT
C	0.11	0.06	0.06	0.05
Mn	2.07	1.68	1.26	1.53
P	0.008	0.018	0.017	0.014
S	0.008	0.007	0.01	0.003
Si	0.09	0.22	0.31	0.25
Ni	2.25	2.05	2.31	2.15
Cr	0.84	0.77	0.86	0.88
Mo	0.71	0.71	0.75	0.70

similar flux, Lincoln 880. A similar result was obtained, both carbon and manganese were reduced and silicon increased. The element reduction was of major concern since both these elements affect the hardenability of the steel. The flux manufacturer suggested that the current density was too high for the wire size load. Another pad was produced using the following welding conditions and the OP121TT flux.

Current	275 A
Voltage	24 V
Travel speed	10 ipm
Primary wire feed	117 ipm
Secondary wire feed	13 ipm
CTWD	1/2 inch
Heat Input	39.6 kj/in.

This resulted in an even greater change in composition. It was anticipated that anything that could be done to lower the ratio of flux consumed to weld nugget area should lower the rate of interaction with the flux. From experience this was known to occur when the current is maximized and the voltage is minimized. A number of welding conditions were developed and chemical analysis pads produced. The welds were produced by varying current, voltage, and travel speed with a heat input in the 40-45 kj/inch range. Indeed, the welding conditions selected with high current and low voltage produced one of the lowest flux consumption rates. These conditions also resulted in the smallest change from the expected composition. Due to the high thermal process efficiency of SAW (when compared to GMAW), it was decided to make the SAW welds near the lower end of the heat input range.

Since the presence of a flux in the welding system introduces the possibility of hydrogen pickup, it was decided to bake the plate out after welding using the treatment specified for GMAW (350F for 12 hours). The final para meters used were:

Current	400 A
Voltage	23 V
Travel speed	13.5 ipm
Primary wire feed	207 ipm
Secondary wire feed	24 ipm
CTTW	1/2 ipm
Heat input	40.9 kj/inch

The welded plate appeared radiographically sound and was subjected to tensile testing. A new plate was then welded conforming to the requirements specified for the dynamic tear test plate. These required a lower heat input situation which was achieved by increasing the travel speed from 13.5 to 16 inches per minute.

A metallographic cross section is shown in Figure 27.
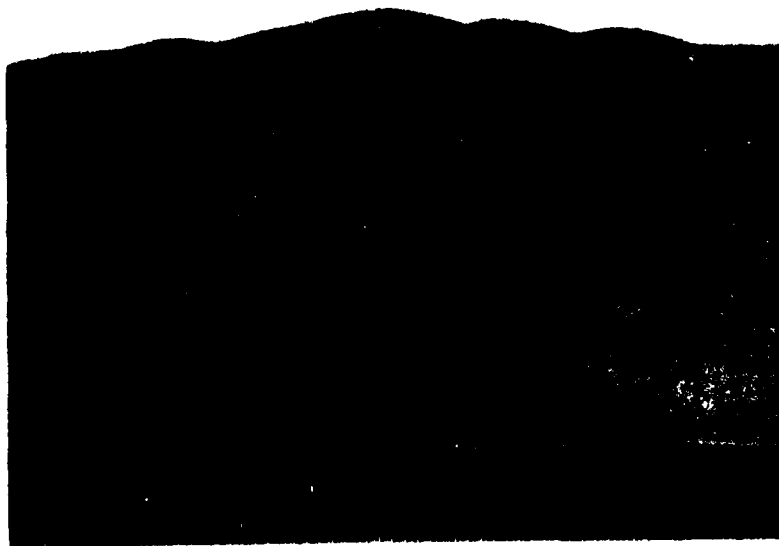
Figure 27. Metallographic cross section of SAW-02

Chemical Composition and Homogeneity

For the systems considered it was necessary to determine both the average (gross) weld metal composition and also the local variations of composition which might arise from inadequate mixing of the component filler metals.

Bulk Chemical Composition of Weld Metal

The procedure used to evaluate the average weld metal composition consisted of the weld pad technique as illustrated in Figure 28. In this technique successive weld beads were placed on an HY-130 plate until it was estimated that dilution effects from the base metal could be ignored. The pad of weld metal was then ground on the top surface to provide an area adequate for three spectrographic determinations.

The analysis was carried out commercially on equipment calibrated daily from standards related to NBS standards. All chemical analyses of this type reported are the average of three determinations. Typical results are shown in Table 11 for the GMAW process and indicate the spread of values that were experienced from different locations in the weld.

Mixing and Homogeneity of Weld Metal

Mixing was evaluated by examining transverse, vertical longitudinal, and horizontal longitudinal cross-sections of welds in two ways. Optical microscopy was used to show gross lack of mixing and the different transformation structures that might be expected if the amounts of Ni, Cr, and Mo varied greatly from one part of the weld to another. Scanning electron microscopy using an X-ray analyzer allowed many points on a selected cross section to be analyzed for chemical composition in a systematic manner, yielding a quantitative estimate of mixing.

Welds were made with various constant levels of secondary wire addition. In another series, the secondary wire addition was stopped during the weld, soon after steady state was attained, to provide a weld bead of declining alloying element composition. Welds were also made with single AX-140 and L-140 filler wires to examine the segregation that normally occurs in these welds.

Transverse cross-sectional specimens about 0.125 in (3 mm) thick were removed from the weld, trimmed to barely include toes and root, and mounted in bakelite. They were ground and polished, etched with 10% ammonium persulfate solution for macrostructural analysis, and repolished and etched with 2% Nital for microstructural evaluation. Selected specimens were repolished and lightly etched for microhardness testing. Specimens selected for chemical analysis by electron microprobe were returned to the microhardness tester, where a grid of indentations was made, as shown in Figure 29. The indentations served as reference marks near which the x-ray analyses would be taken. These specimens were then repolished (the indentations remained visible) to provide a smooth surface for accurate microprobe determinations, sprayed with clear acrylic for protection, removed from their bakelite mounts, and cemented to the stubs that adapt them to the stage of the

TABLE 11. TYPICAL RESULTS OF SPECTROGRAPHIC ANALYSIS FROM
VARIOUS LOCATIONS ALONG A GMA WELD PAD AT TWO HEAT INPUTS

	Ni	Cr	Mo
Heat Input -- 45kj/in.	2.23	1.18	0.86
	2.29	1.16	0.86
	2.16	1.08	0.83
	2.21	1.09	0.85
Mean	2.25	1.13	0.85
Heat Input -- 35kj/in.	2.21	1.04	0.81
	2.20	1.05	0.82
	2.39	1.19	0.85
	2.31	1.14	0.83
Mean	2.28	1.10	0.83
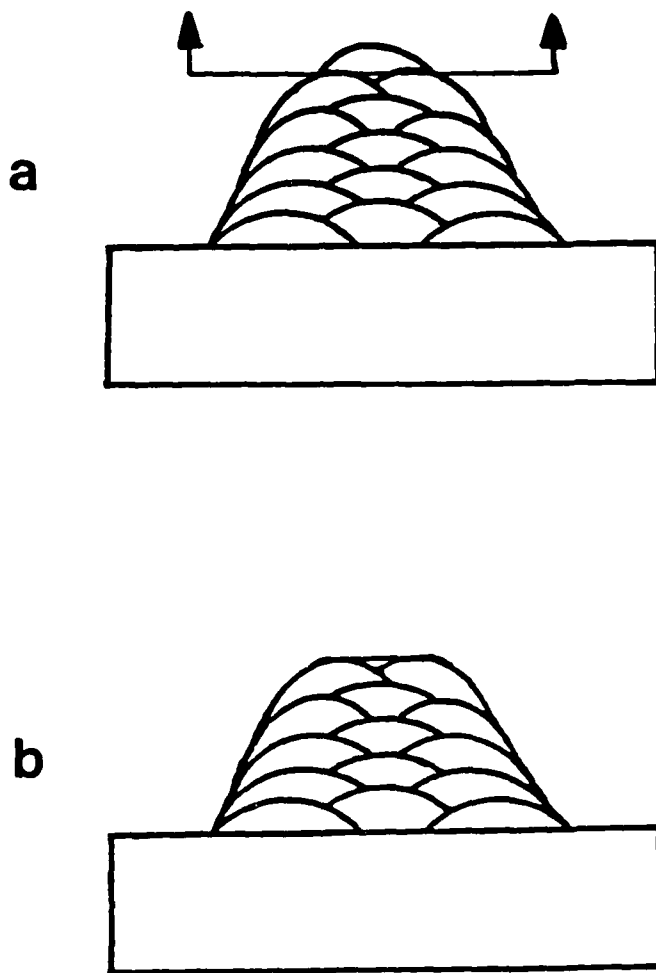
Figure 28. Schematic illustration of chemistry pad buildup.

(a) buildup is produced using bead on plate technique,
then top surface is milled flat

(b) top surface is essentially all filler metal and is
subjected to spectrographic analysis
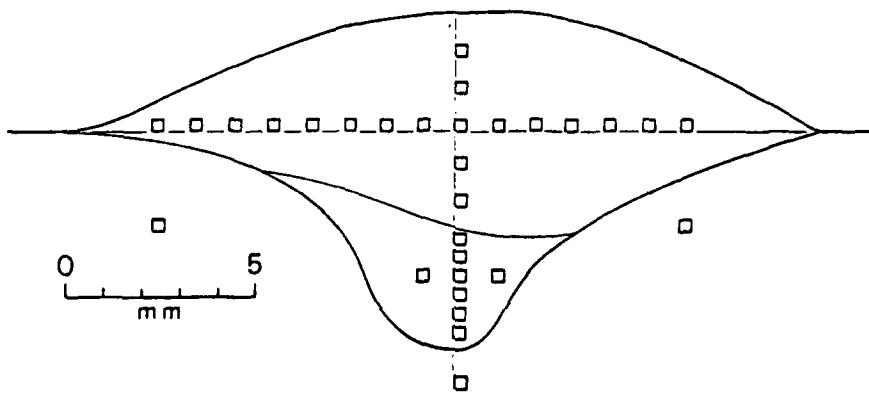
Figure 29.   Typical microprobe analysis pattern for welds.

electron microscope. The acrylic was removed with acetone immediately prior to insertion into the microscope.

X-ray Analysis in the
Scanning Electron Microscope

The instrument used for this phase of the work was the Cambridge S4-10 Scanning Electron Microscope. Attached to the microscope is an Ortec X-ray analyzer. Since the electronic structure of each chemical element is unique, the X-rays that are emitted after the specimen's electrons are disturbed by the high-energy electrons of the SEM beam have a unique energy distribution that identifies that element. In the X-ray analyzer, a solid-state detector located near the specimen is exposed to the X-rays emitted by electron beam/specimen interactions and separates them into an energy spectrum that is electronically divided into 2048 channels, each of which is then counted separately. The output includes a Bremsstrahlung background curve, caused by the acceleration of the electrons as they move through the material. Superimposed on this background are the energy peaks corresponding to beam interactions with inner shell electrons (see Figure 30). Quantitative analysis is possible if the background is subtracted out, the area under the peaks computed, and peak heights corrected for such effects as absorption and fluorescence. The Colby MAGIC4 computer program does this automatically given peak heights, background levels, and a standard analyzed by other means.

The specific procedure followed in this work included the following steps, summarized in Figure 31. The specimens were mounted in the SEM and the area to be analyzed and was found and focused. The analysis covered an area large enough to overcome interdendritic segregation effects, generally a 7 x 7 cm raster at 200X, which on the specimen is roughly 0.3 mm (0.012 in) on a side. The analyzer was activated and counted the emitted X-rays for 40 or 80 seconds. The "Region of Interest" switch on the analyzer was used to select segments along the background curve and across the elemental peaks of interest.

The teletype terminal was activated and the count values for these regions of interest were printed out; identification and location data about the specimen were manually typed onto the printout, and the next sample point could be analyzed. In order to increase the X-ray flux reaching the detector, the sample is tilted relative to the beam; in order to keep the specimen/detector geometry constant, this necessitates focusing mechanically by moving the specimen up or down rather than electronically by changing the beam parameters. At some point in the run the base metal, a chemically analyzed known standard of HY-130, was counted in the same fashion. The banding due to segregation in HY-130 plate was observed to be on the order of 0.05 mm (0.002 in), so that the 0.3 x 0.3 mm (0.012 x 0.012 in) analysis area averaged the composition as thoroughly as the 3 mm (0.12 in) diameter spot of the spectrographic analysis.

After this procedure, the data were reduced for input to the Colby MAGIC program. This involved selecting from the teletype output an average background for each peak and subtracting it from the peak height, creating from this an input file for the computer. An example of such a file is shown in Figure 32, along with its output format. Of interest in the HY-130 system
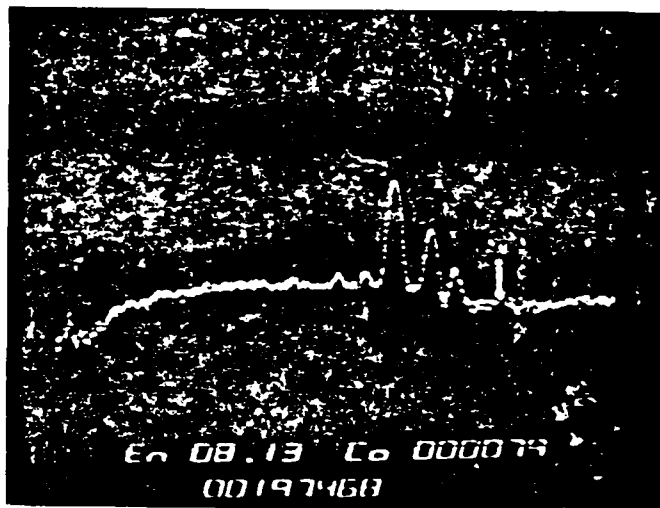
Figure 30. Typical X-ray energy spectrum for HY-130. The hump at the left is due to the Bremsstrahlung radiation, while the peaks are due to characteristic energy levels for individual elements.
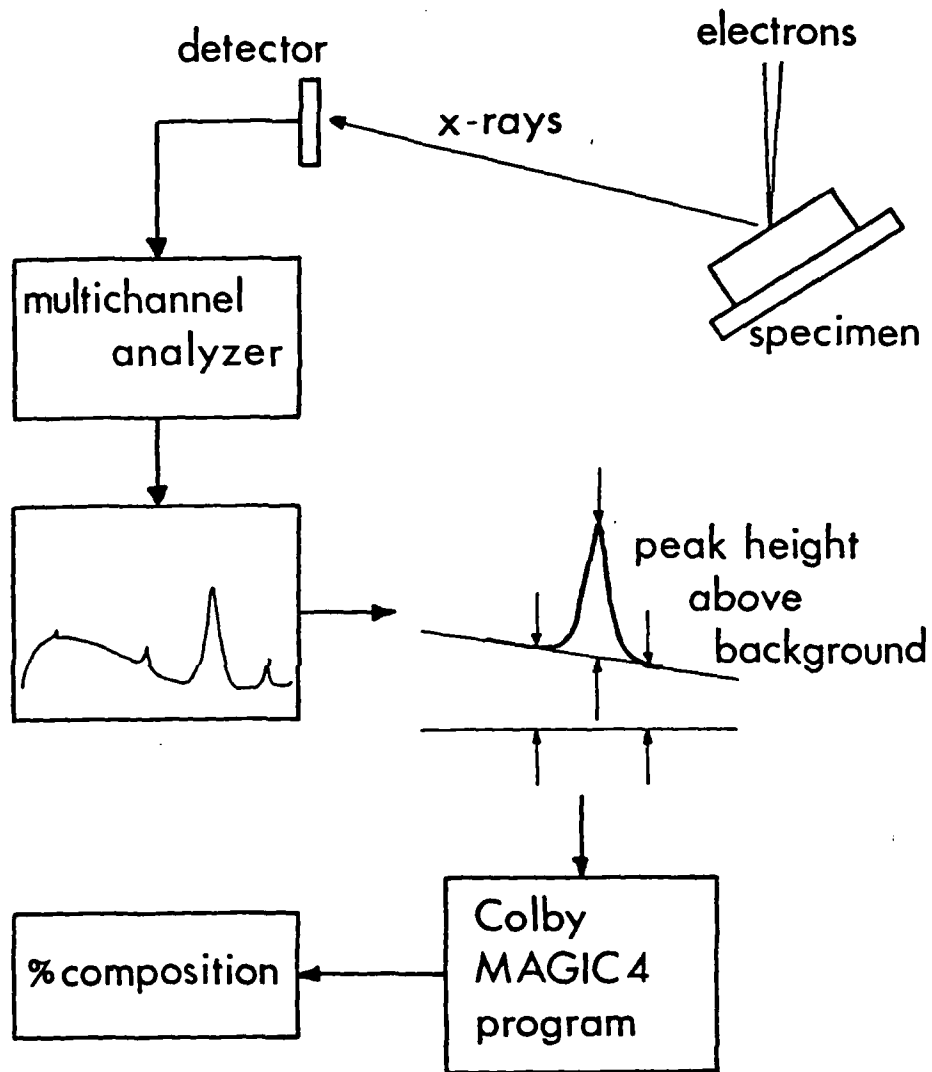
Figure 31. Schematic procedure for obtaining quantitative analyses from the Scanning Electron Microscope. The "peak height above background" step is done using numerical values of the approriate channels from a Teletype output.

63

```
180001  SEC WIRE CFF TRAV       DATE 26 JAN 83
20.0  4            20.
CR KA   MN KA   FE KA   NI KA
1.9234FE.0086MN.0503NI.0055CR.0053MO.0010CU
2.9234FE.0086MN.0503NI.0055CR.0053MO.0010CU
3.9234FE.0086MN.0503NI.0055CR.0053MO.0010CU
4.9234FE.0086MN.0503NI.0055CR.0053MO.0010CU
      71.        49.       40.        73.       49.      40.     870 08
      84.        49.       40.        71.       48.      40.     870 08
    2607.        45.       40.      2651.       46.      40.     870 08
      68.        24.       40.        94.       29.      40.     870 08
      75.        47.       40.                           40.     856 14
      79.        46.       40.                           40.     856 14
    2523.        43.       40.                           40.     856 14
      68.        25.       40.                           40.     856 14
      72.        48.       40.                           40.     869 91
      85.        48.       40.                           40.     869 91
    2618.        43.       40.                           40.     869 91
      64.        27.       40.                           40.     869 91
=2.0
POINT 4.4

SUBMITTED BY: SEC WIRE OFF TRAV

DESCRIPTION: POINT 25.0

            MEAN CHEMICAL COMPOSITION AND TWO
            SIGMA LIMITS BASED ON    3 ANALYSES

                        WEIGHT          ATOMIC




ELEMENT      PERCENT            PERCENT

  CR       0.42 + 0.06        0.43 + 0.08

  MN       1.38 + 0.0         1.34 + 0.06

  FE      95.17 + 4.16       94.70 + 0.29

  NI       3.89 + 0.59        3.52 + 0.39
```

Figure 32. Input and output formats of the Colby MAGIC4 program.

are Fe, C, Mn, Si, P, S, Ni, Cr, Mo, and minor residuals and tramp elements. For various reasons, some of these elements are more readily detectable than others. The Mo peak used for analysis is the L alpha, which happens to lie at the same energy as the S K alpha peak. The amount of S in this system is very small compared with the Mo, and on the relatively large scale analyzed here (thus avoiding microsegregation) should not enter into the analysis; however, the background at this energy is high and quite nonlinear. The X-ray emission of C is at a very low energy and it cannot be analyzed on the system used.

Eliminating Mo because of background problems and its identity with S on the spectrum, the most prominent remaining peaks on the spectrum are those of Cr, Mn, and Ni. These elements were chosen as markers. The primary wire is rather high in Mn but low in other alloying elements; the secondary wire is very high in Ni and Cr. The base metal is higher in Ni but lower in Cr and Mn than the nominal weld composition, which is a perfect mixture of primary wire, secondary wire, and diluted base metal. A spot in the weld with high Ni and low Mn and Cr could be interpreted as unmixed base metal, a spot with high Mn but very low Ni and Cr as unmixed weld metal from the primary wire, a spot with very high Ni and Cr was unmixed secondary wire, and so forth. These criteria are quantified in Table 12.

TABLE 12. INDICATOR COMPOSITIONS FOR MICROPROBE ANALYSIS
OF GMAW DEPOSIT
(Weight Percent)

	Mn	Ni	Cr
HY-130	0.89	5.03	0.55
E80S-D2	1.60	0.17	0.072
Hastelloy X	0.60	46.7	21.98
Ideal Mixing: 96% E80S-D2 4% Hastelloy X 55% Dilution by HY-130	1.19	3.68	0.73

WELDING CONDITIONS FOR MECHANICAL TEST PLATES

With each of the three welding processes, considerable optimization of welding conditions was needed to ensure optimum bead shape and operating characteristics. The conditions used for preparing the mechanical test specimens are given in appendix A for each of the three processes.

MECHANICAL TESTING

The mechanical properties of welds produced with all three processes were evaluated, and these were compared to the appropriate MIL-specification. The properties of interest were:

o All weld metal tensile tests

o Dynamic tear testing – 5/8 inch specimens

The properties to be met are outlined in MI30CE/2 and MILE24355A(SHIPS) for shielded metal arc and gas metal arc, respectively. Since there is no specification for submerged arc welding, the gas metal arc requirements were used for comparison. In addition,hardness and bend tests were carried out for the purposes of assessing toughness, ultimate (and hence yield) strength and ductility on a preliminary basis.

Tensile Testing: Tests were carried out by Midwest Testing Laboratories, Inc., Piqua, Ohio, in accordance with ASTM-A370. Yield strength was assessed on the basis of 0.2 percent offset in a gage length of 2 inches.

Dynamic Tear Testing: Samples of all welds were machined "in house" to MIL-STD1601(SHIPS) and were tested at DTNSRDC, Annapolis, Maryland.

Other Testing: Hardness and bend ductility tests were carried out "in house".

RESULTS AND DISCUSSION

The objective of the program was to examine the feasibility of synthesizing the weld metal composition of high strength steel weld metal by mixing two metallic components in the weld pool. This was accomplished for three commonly used welding processes:

> Gas Metal Arc Welding
> Submerged Arc Welding
> Shielded Metal Arc Welding

To accomplish the objective, a mechanical system for introducing the two components into the weld pool was needed and a high degree of mixing of the two was required in the weld pool . Success in these tasks was to be evaluated by achieving suitable mechanical properties of the weld metal. The results and discussion are presented along these lines.

System Development

The SAW and GMAW processes are similar in nature. A continuously fed solid wire is fed into the arc zone and forms the anode of the arc. Metal transfers from the end of the wire to the pool to provide a source of filler metal. The GMAW process is gas shielded (argon-2% oxygen for high strength steel welding); the SAW process is shielded by flux (normally a neutral flux with high basisity).

The economic advantages of using commercially available filler wires for the above processes, in lieu of specially alloyed filler wires designed to provide weld metal chemical compositions suitable for the base metal, are great. Therefore, a system was designed to feed two commercially available wires; one to maintain the arc and to provide the majority of the filler metal and the second wire to provide the essential alloying elements. Both wires were fed to the arc by conventional wire feeders at speeds of appropriate proportions to achieve the overall desired composition of the weld metal. It was shown that subtle changes in weld metal composition could be obtained by making small adjustments to the feed rate of the second wire. This could be very useful if, for example, the alloy content and, hence, the hardenability of the weld metal, needed to be increased to compensate for lower cooling rates.

In the SMAW process, the system is not so versatile. Hence, the proportions of metallic components are not continuously variable, but must be in fixed predetermined ratio since the electrode main wire and the secondary wire melt at the same rate. In this program the second "wire" consisted of either a core of high alloy at the center of the rod or a strip of high alloy content tacked to the surface of the rod. As the electrode melts, the two melt in proportion to produce a weld metal of the desired composition. The coating of the electrode provides the normal functions: arc stabilization, wire powder addition, deoxidation and gas shielding. However, the alloying elements are not included in the coating.

For all three processes, GMAW, SAW and SMAW, it was found possible to reproduce closely, by the synthesizing technique, the gross chemical composition of weld metal obtained by the more conventional practices.

In the case of SMAW, the microscope homogeneity of the weld metal was equal to or better than that of the conventional technique whereby the alloying elements are added to the pool via the electrode coating in powdered form. For SAW, the homogeneity of the weld metal was judged excellent. However, for the GMAW process there were notable inhomogeneities in the chemical composition of the weld bead, particularly in the region of the deep penetration "finger."

Chemical Composition and Homogeneity of the Weld Metal

Considerable effort was expended to examine the composition and homogeneity of weld metals for HY-130, produced by the GMAW and SMAW processes. As mentioned earlier, the SEM technique was used for local analysis in addition to spectrographic analysis for gross composition.

Gas Metal Arc Welding

Using a cold wire feed of the second wire to the leading edge of the pool the results of weld pad deposit analyses for Linde 44 and E80S-D2 main wires for various levels of Hastelloy 'X' addition are shown in Table 13 and 14 and plotted in Figures 33 and 34. There was considerable scatter for E80S-D2 samples which, on further investigation, turned out to be due to an inhomogeneous weld bead. Half the bead (divided on the vertical longitudinal plane) had substantially higher alloying element contents, though the average of 6 or 7 shots produced values close to the expected. The Linde 44 system showed good agreement at the higher levels of Hastelloy addition, but a uniformly high composition at the lowest addition level. The analyses showed little scatter, so that the outliers must have been due either to a mistaken setting during welding or, possibly, to having been taken all on the same side of a dividing line like that seen in the E80S-D2 sample. Segregation was not apparent metallographically.

The most obvious lack of mixing of the secondary wire occurred near weld starts. There was a delay, often of up to one second, but occasionally of several seconds, in the establishment of stable spray-transfer conditions in the arc. During this time, the weld pool oscillated violently and irregularly, and the distribution of the secondary wire material was poor (Figure 35).

Under stable welding conditions this improved, but unmixed regions were still observed occasionally. Two welds were examined in detail for homogeneity

E-80S-D2 with Hastelloy X and
E-80S-D2 (no Hastelloy)

Optically, the differential etching of the finger penetration region is very obvious when the Hastelloy is added (Figure 36). In figure 37, a plot of composition versus distance from the top surface, shows a drastic change in Ni and Cr content in the deep penetration zone (darker-etching region). The Mn stays constant or rises slightly. These effects are consistent with welding conditions in which the Hastelloy is effectively shut out of the finger penetration zone, leaving a mixture of primary wire and base metal.

70

TABLE 13. CHEMICAL ANALYSIS PAD RESULTS FOR VARIOUS LEVELS
OF SECONDARY WIRE ADDITION

LINDE 44/HASTELLOY X
(Weight Percent)

Hastelloy X
addition:

Percent of Deposit	2.9	3.8	4.7
Wire Feed Speed (in./min.)	19	25	31
C	0.10	0.11	0.10
Mn	2.04	1.98	2.02
Si	0.052	0.048	0.054
P	0.012	0.013	0.013
S	0.013	0.014	0.013
Ni	2.59	2.41	2.69
Cr	0.99	0.88	1.01
Mo	0.80	0.76	0.80
Co	0.109	0.099	0.112
Cu	0.27	0.26	0.26

Note---0.035 in. wire

TABLE 14.   CHEMICAL ANALYSIS PAD RESULTS FOR VARIOUS LEVELS
OF SECONDARY WIRE ADDITION

E80S-D2/HASTELLOY X
(Weight Percent)

Hastelloy X
Addition:

Percent of Deposit	3.2	4.0	4.7
Wire Feed Speed (in./min.)	20	25	30
C	0.063	0.067	0.067
Mn	1.64	1.67	1.67
Si	0.53	0.54	0.54
P	0.012	0.013	0.012
S	0.016	0.017	0.017
Ni	1.57	1.90*	2.40*
Cr	0.79	0.96*	0.67*
Mo	0.67	0.69*	0.78*
Co	0.077	0.088*	0.107*
Cu	0.35	0.33	0.33

Note--- 0.035 in. wire

*Indicates average of 7 spark burns taken to overcome scatter
caused by inhomogeneity from two-cell circulation patterns; see text.
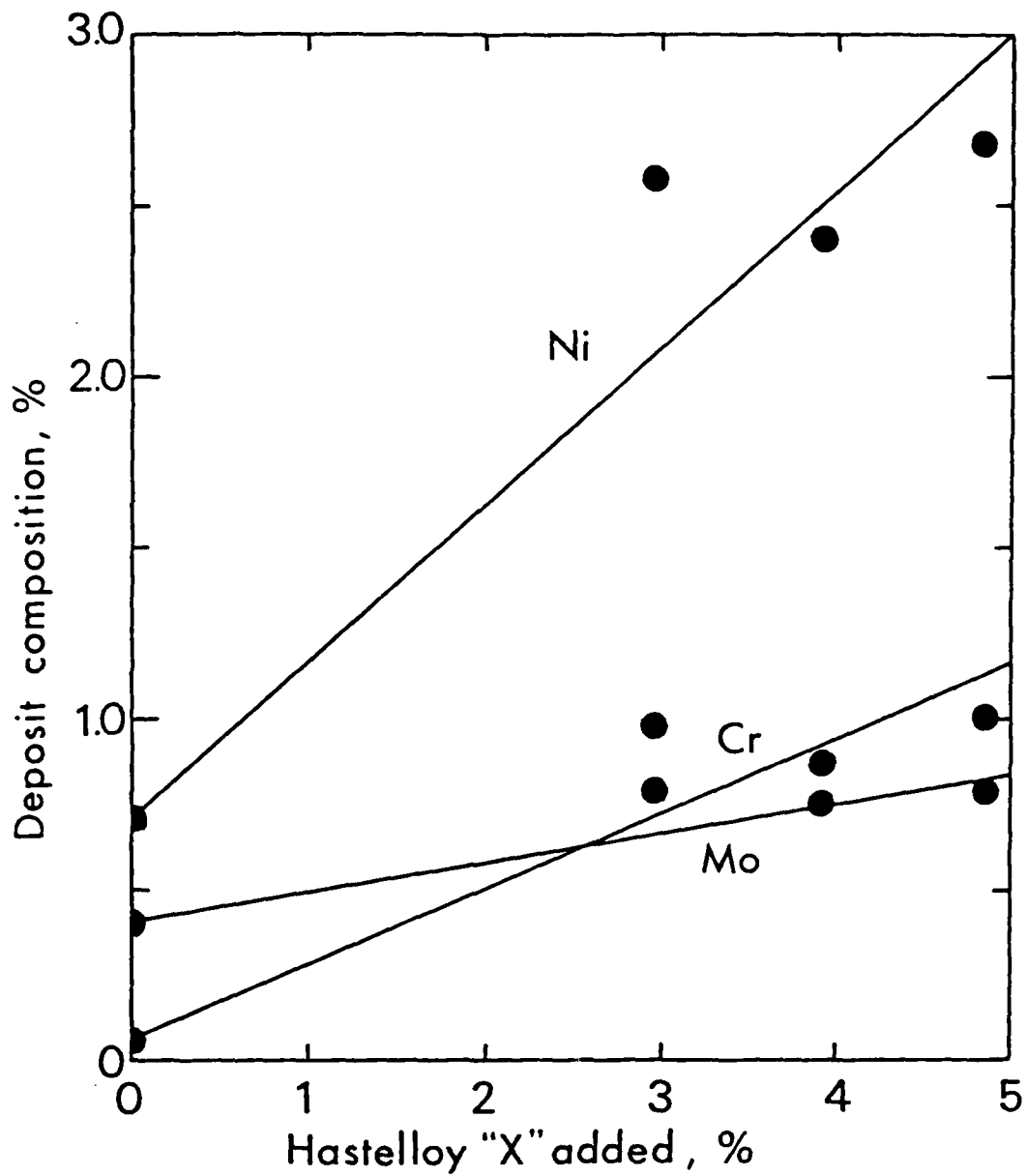
Figure 33. Results of weld metal chemical analysis from Gas Metal Arc, method 1, pad deposit. Linde 44 with various additions of Hastelloy 'X'. Spectrographic analysis compared with calculations.
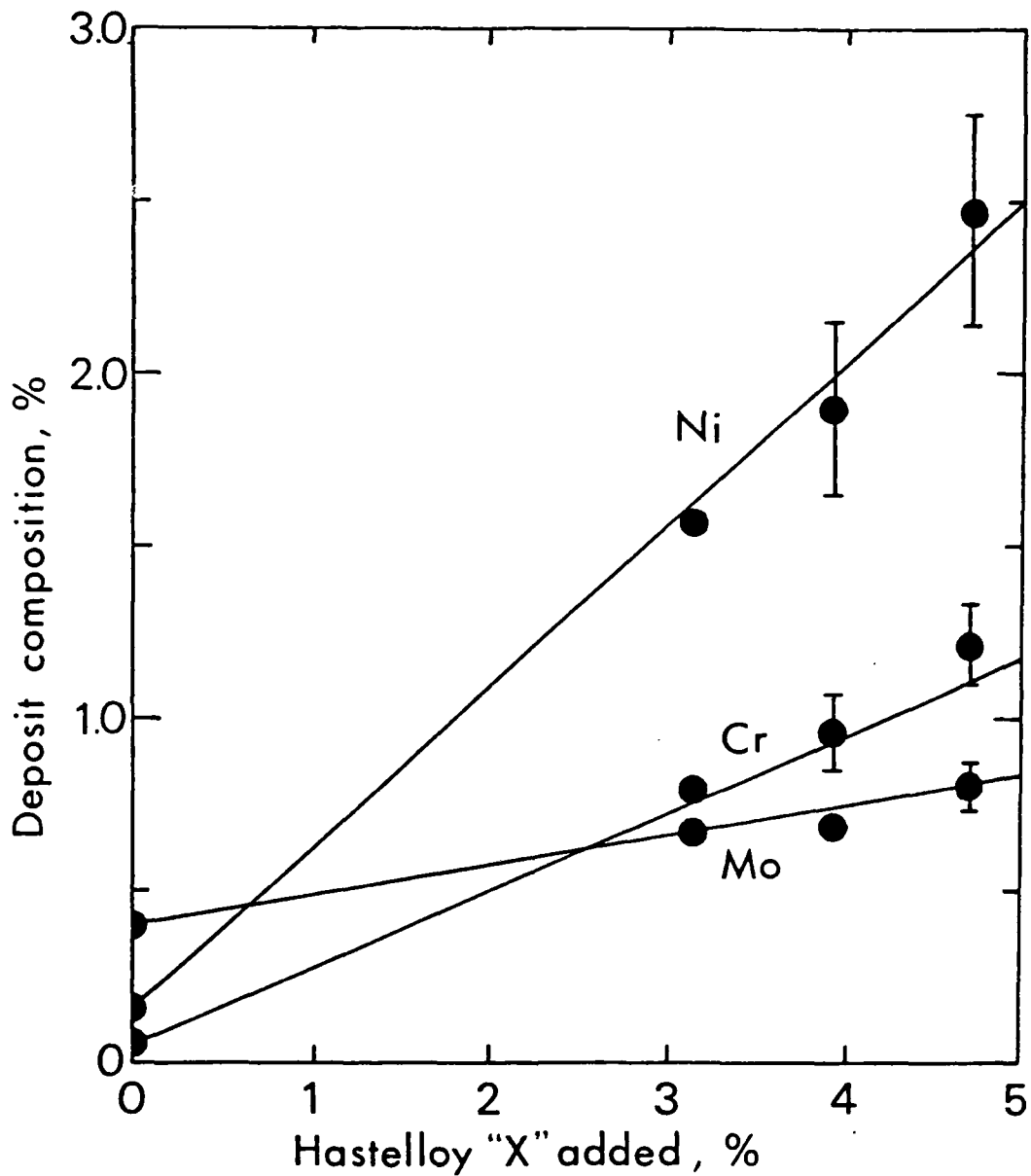
Figure 34. Results of weld metal chemical analysis from Gas Metal Arc, method 1, pad deposit. E80S-D2 primary wire with various additions of Hastelloy 'X'. Spectrographic analysis, compared with calculations. Bars indicate 2-sigma limits of 7 analyses at different points in the deposit. Scatter is evidently due to 2-cell mixing pattern.
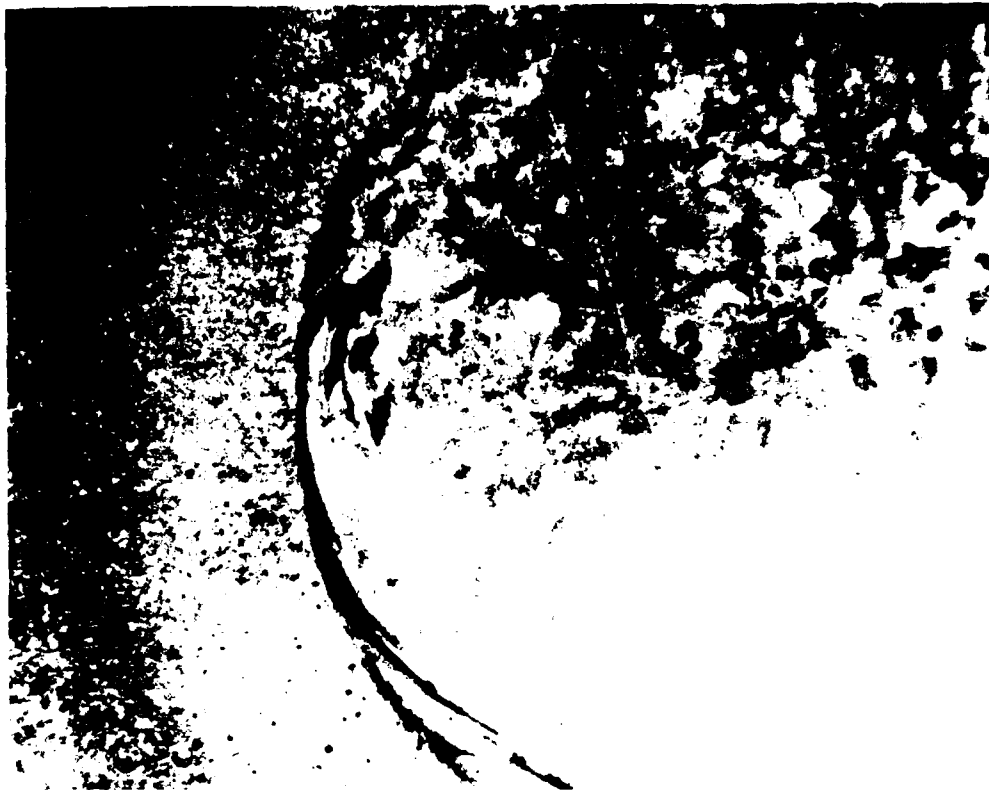
Figure 35. Pure Hastelloy 'X' (dark) at the beginning
of a Gas Metal Arc weld (method 1), illustrating the
gross lack of mixing that can occur before stable
welding conditions are achieved. Weld reinforcement
was ground off to plate level. (9X, 2% Nital)

Figure 36. Transverse cross section of a Gas Metal Arc weld (E80S-D2 and Hastelloy 'X') showing the differential etching of the finger zone. (8X, 2% Nital)
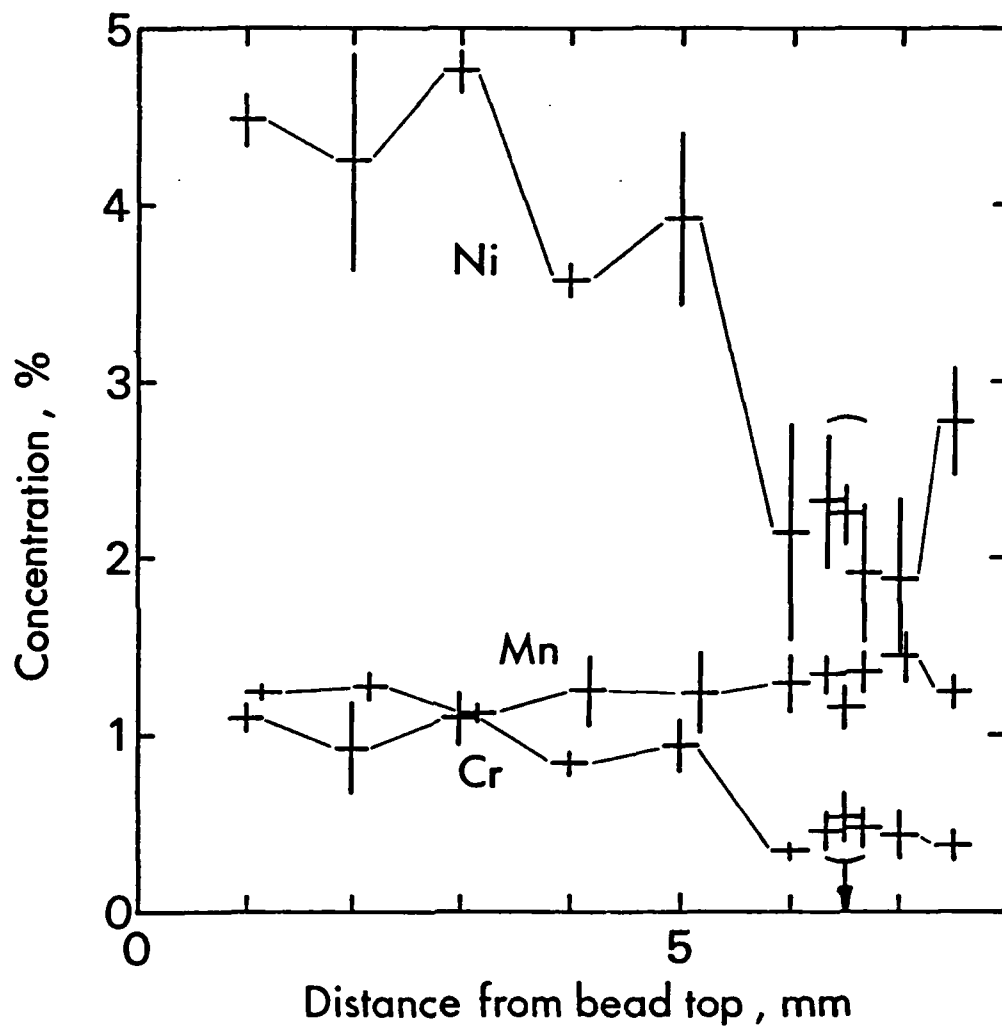
Figure 37. Vertical traverse of a Gas Metal Arc, method 1, weld produced using E80S-D2 primary wire and Hastelloy 'X' secondary wire on HY-130 base plate. Dark etching finger region shows much lower Nickel and Chromium levels but equivalent Manganese content, indicating that it consists mostly of unmixed primary wire. Point farthest to the right includes some base metal in the analysis area. Bars indicate 2-sigma limits.

Figure 38 is an X-ray analysis traverse across the same weld at plate level. It shows in detail the same inhomogeneity that affected the weld pad deposits analyzed spectrographically and mentioned above. On the right side, the Ni and Cr are substantially elevated, while the Mn remains approximately constant. Figure 39 offers a possible explanation for this. The droplets forming the finger penetration (Figure 40) cause outward flow on all sides of the central depression in the weld pool, and force the incoming Hastelloy out around it. Only if the placement of the secondary wire is very precise would the flow divide evenly. The Hastelloy is subject to mixing and diffusion as it moves from front to rear, but there is evidently a two-cell circulation, like that described by Woods and Milner(11), operating in the rear part of the pool, which preserves any imbalance.

The weld, made without Hastelloy, sheds additional light on this process. There was no differentially etched zone, but in the vertical traverse (Figure 41) the Ni and Cr contents still fall and the Mn content still remains constant. In this case, however, without Hastelloy, the change represents changing dilution conditions. The upper part of the weld shows about the levels expected, while the layering in the less equilibriated finger zone shows substantially higher levels of filler metal. Segregation of alloying elements must therefore be expected in the GMA weld beads, particularly related to the deep penetration finger, when a dissimilar metal is added to the leading edge of the weld pool.

For this reason, further work was carried out, by adding the second wire adjacent to the main electrode at the top of the arc. In this way the two wires melt together and some mixing occurs before and during transfer through the arc. Both cold wire feed (Method 2) and "hot" wire feed (Method 3) were used.

Spectrographic analysis of weld pads made with these methods showed that a much more uniform weld metal composition is produced. The only observed disadvantage of feeding the secondary wire at the top of the arc was that there was a small reduction of alloy transfer efficiency. This could, of course be compensated for by a slight increase in the rate of feed of the wire.

Shielded Metal Arc Welding

Optical examination of the SMAW welds made with composite and conventional E14018 electrodes showed few differences, although three distinct types of heterogeneities were observed.

In the conventional E14018 deposit, several light-etching inclusions were discovered. A typical example appears in Figure 42. Qualitative X-ray analysis on the SEM (Figure 43) indicates that the inclusion is rich in molybdenum. This corresponds well with the findings of Gouch and Muir (6) and Erokhin (12) who also found alloying elements from the coating segregated in the weld metal. The fact that several were found in the relatively few cross sections taken means they are probably quite common in the deposits made with this electrode. These molybdenum rich bands are thought to result from unmixed ferromolybdenum powder, and were not detected in similar composite electrode deposits.
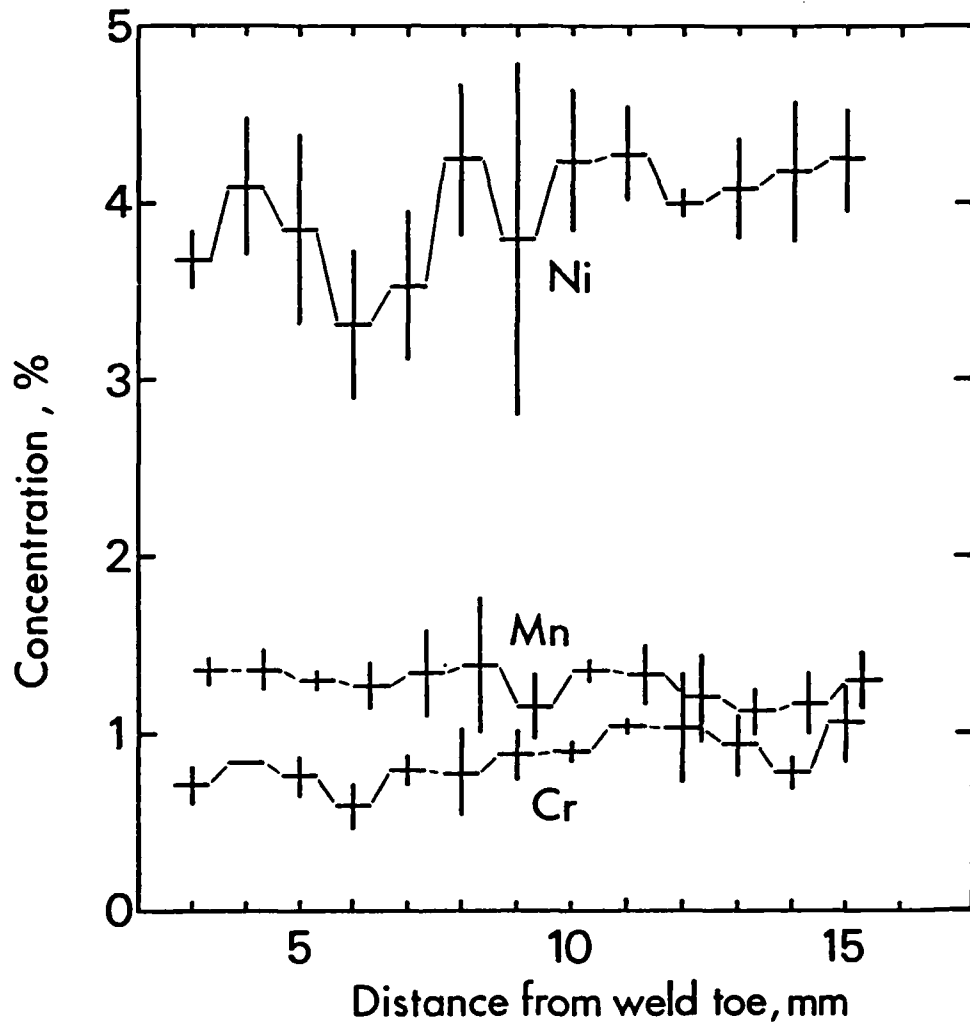
Figure 38. Horizontal traverse of a Gas Metal Arc, method 1, weld produced using E80S-D2 primary wire and Hastelloy 'X' secondary wire on HY-130 base plate. Note the higher Nickel and Chromium (but level Manganese) concentrations to the right, indicating an unequal division of the melted secondary wire and a 2-cell circulation pattern behind the arc, at least at plate level. Bars indicate 2-sigma limits.

79
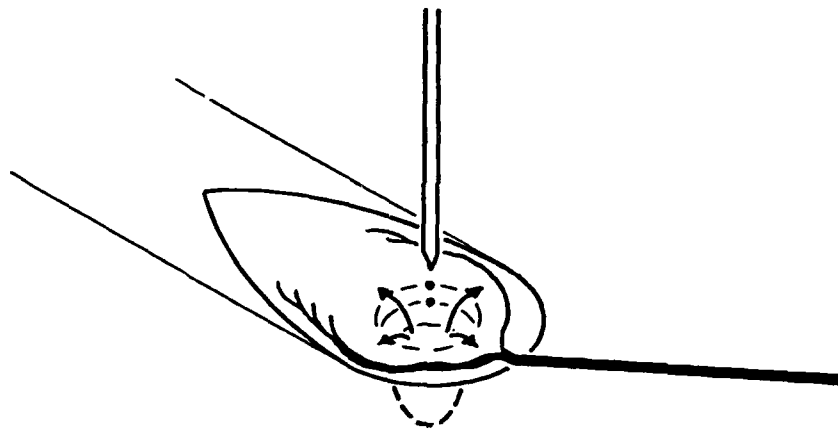
Figure 39. A possible mechanism for the distribution of
melted secondary wire. The outward movement from the
droplet impingement zone divides the secondary material,
probably unevenly, and 2-cell circulation behind the arc
preserves the division.
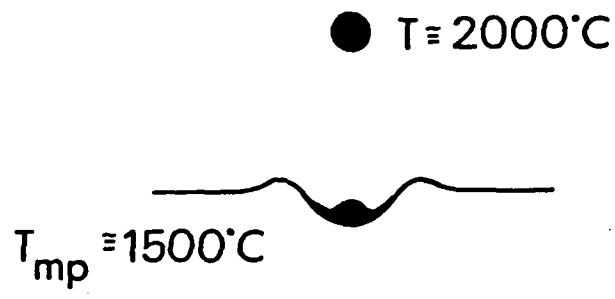
Figure 40. A possible inferred penetration mechanism in Gas Metal Arc welding. The superheated droplet transfers its heat and momentum to the base metal, resulting in deep penetration.

81
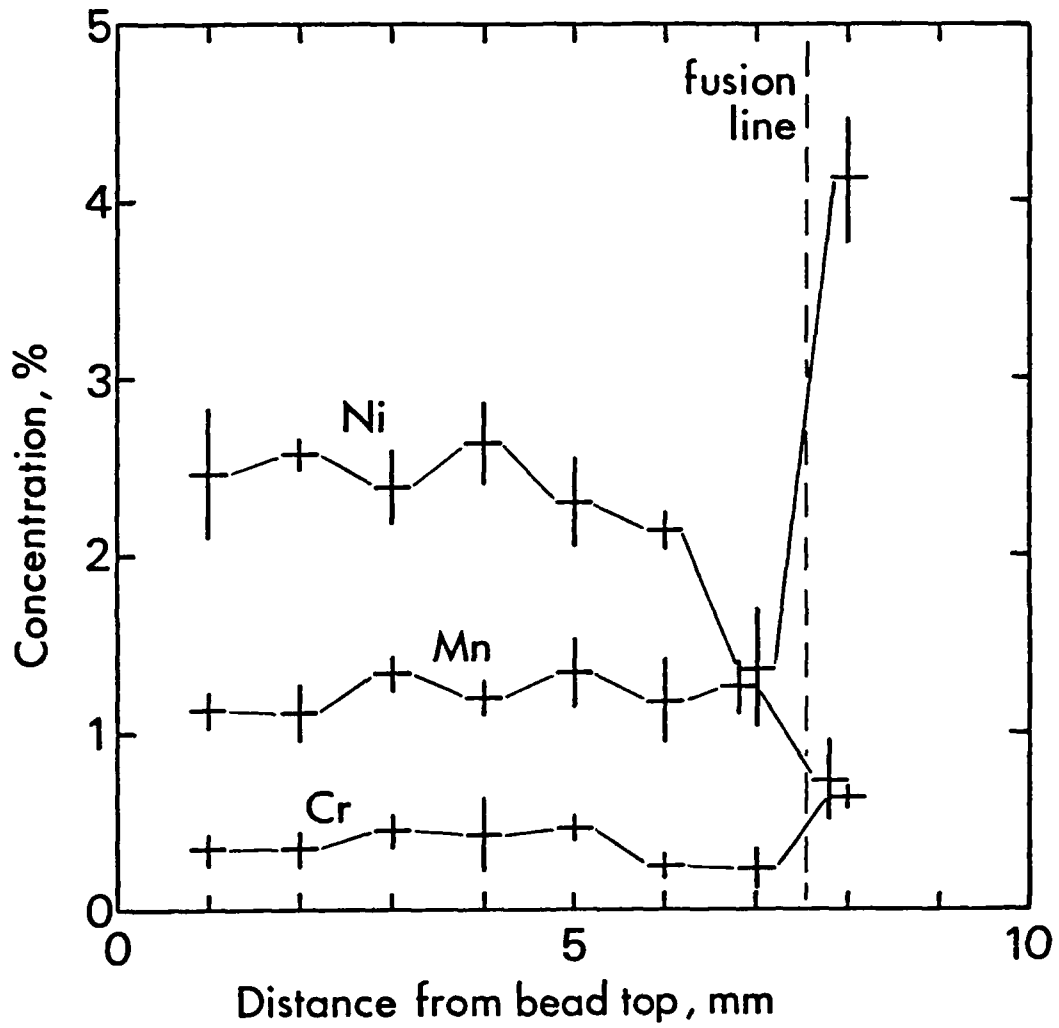
Figure 41. Vertical traverse of a weld made with E80S-D2 only on HY-130 base plate. Nickel and Chromium drop off in the finger zone. Bars indicate 2-sigma limits.

82

Figure 42. The toe area of an E14018 weld showing segregation, which qualitative X-ray analysis shows to be enriched in Molybdenum. (100X, 2% Nital)
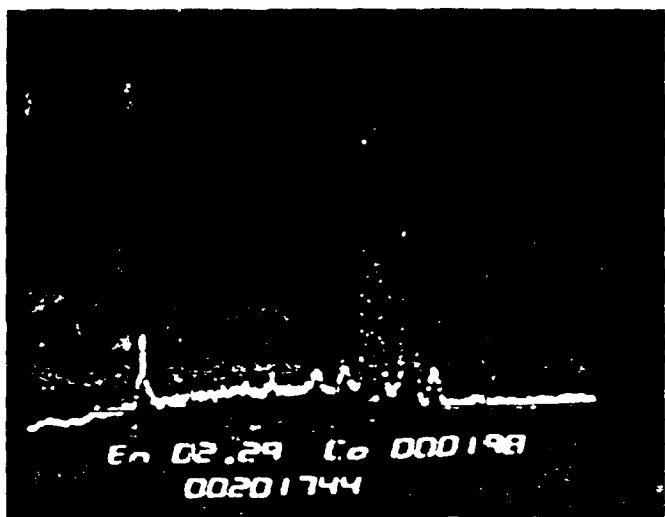
Figure 43. X-ray spot analysis spectra of weld in figure
42, with the cursor set on the 2.29 keV peak characteris-
tic of Molybdenum. Top: small spot on band. Bottom: wider
beam in the weld metal.

Light areas near the fusion line were observed in both types of deposits, and typical examples are shown in figures 44,45, and 46. These regions are better attributed to interleaving with the base metal. This is a fairly common occurence in many types of weld deposits.

Figure 47 is a plot of composition versus distance for a conventional E14018 electrode. There is some variation in nickel content, though there is considerable scatter in the analyses. Figure 48 is a similar analysis of a ribbon-type composite electrode deposit, welded with the ribbon held to the side. This traverse also exhibits variation in the nickel content. Figure 49 shows the results of a traverse across a light-colored band (Figure 50) in a weld made with the Hastelloy ribbon held to the front during welding. The cyclical pattern in nickel concentration may be real and due to the changes in solidification conditions that presumably caused the band, which corresponds to a former weld pool boundary. Another light-colored band (Figure 51) near a weld start was analyzed, and the results, compared with darker-etching weld metal, are shown in Table 15. Slightly higher Mn and Cr are indicated, but the composition is actually quite close. These results indicated that SMAW deposits in general may be prone to the formation of alloy segregated zones.

Mechanical Properties of Weld Metals

Weld metal, from each of three processes, was evaluated for mechanical properties. All-weld-metal tensile and dynamic tear tests were performed, the latter at two temperatures, 30F and 100F. The results are summarized in Table 16. Throughout the program, bend tests (3t) and hardness testing were performed for screening purposes. (Figure 52)

For weld metals of all three processes, yield strengths meeting the minimum requirements of 135,000 psi were readily obtained. In fact, the high yield strengths (all greater than 140,000 psi) probably influenced, in a deleterious manner, the values of ductility and toughness measured.

Test weldments produced with all three processes adequately met the minimum requirement of 14 percent elongation. The ductile fracture appearence of the GMA weld is shown in figure 53. and is typica⊥ of the specimens tested. The exception to this was the initial test plate welded with GMAW, which exhibited a higher than desired yield strength and poor ductility. The high yield strength was attributed to an overmatched alloy content and the poor ductility was probably due to the porosity and hydrogen induced cracking. For the final test plate the alloy content was reduced slightly to lower the strength level, and the welding parameters were altered to reduce the porosity. While this resulted in satisfactory properties, the source of porosity and hydrogen was never determined. One possible source would be contaminants in the consumables, such as those in the copper coating on the main wire.

The dynamic tear toughness values were also variable. The highlight was that the submerged arc weld performed to almost meet the minimum required 500 ftlbs. Therefore the system, in essence, met all minimum requirements using only commercially available welding consumables. Dynamic tear speci-mens for the SA weld at 30F and 100F are shown in figures 54 an. 55, respectively. The SMA weld did not perform as well. Specimens tested from the flat position weld gave a mean value of 115 ftlbs at 30F. At 100F,

85
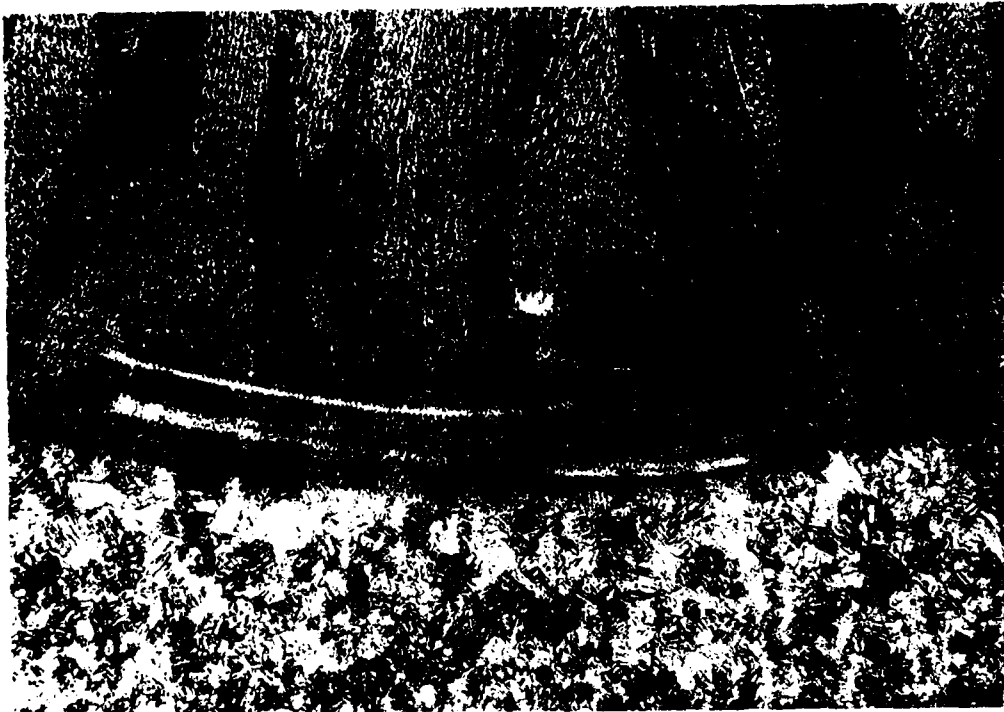
Figure 44. The fusion line of an E14018 weld, showing detached bands of base metal (lighter etching). (28X, 2%
Nital)
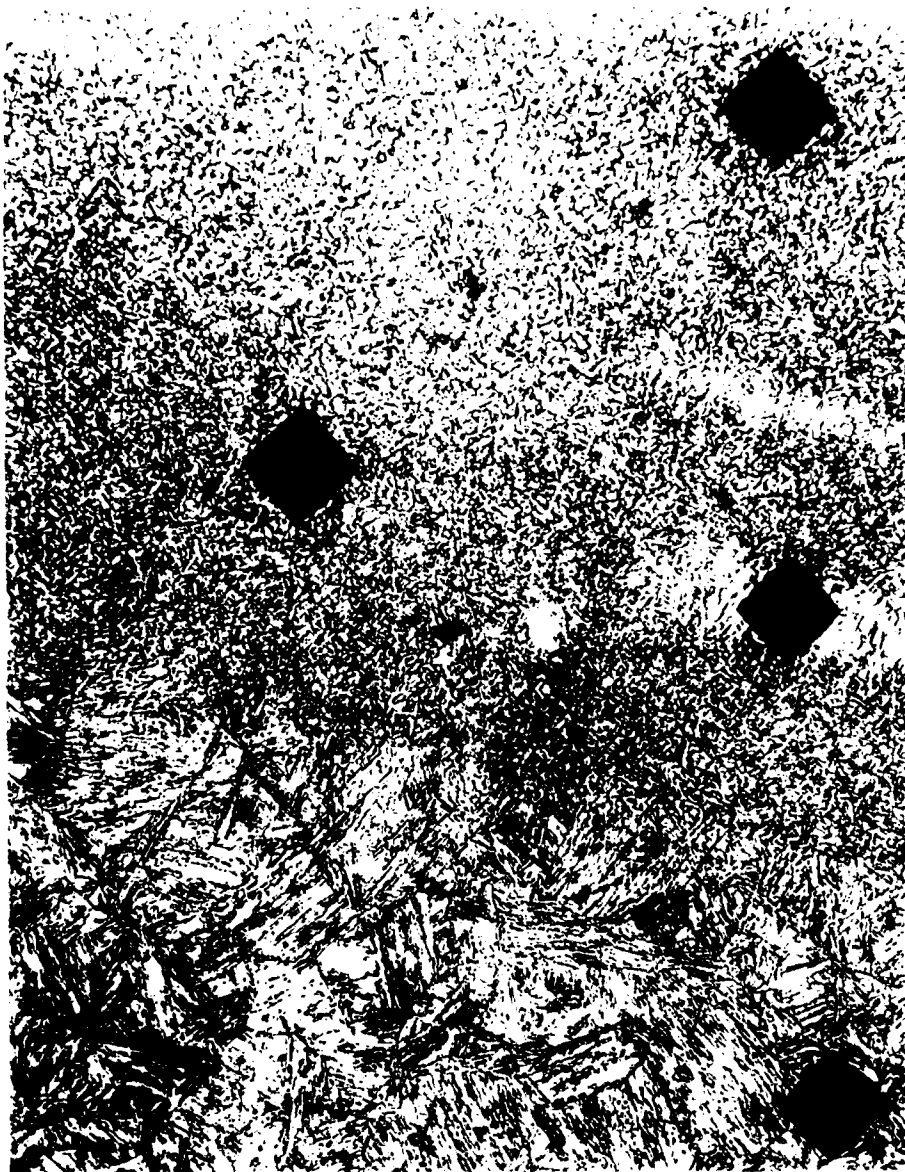
Figure 45. A higher magnification view of figure 44, showing microhardness indentations corresponding to about Rc 32. The indentation to the left is at the same distance from the fusion line as the streak, but shows a hardness like that of the weld metal above. (230X, 2% Nital)
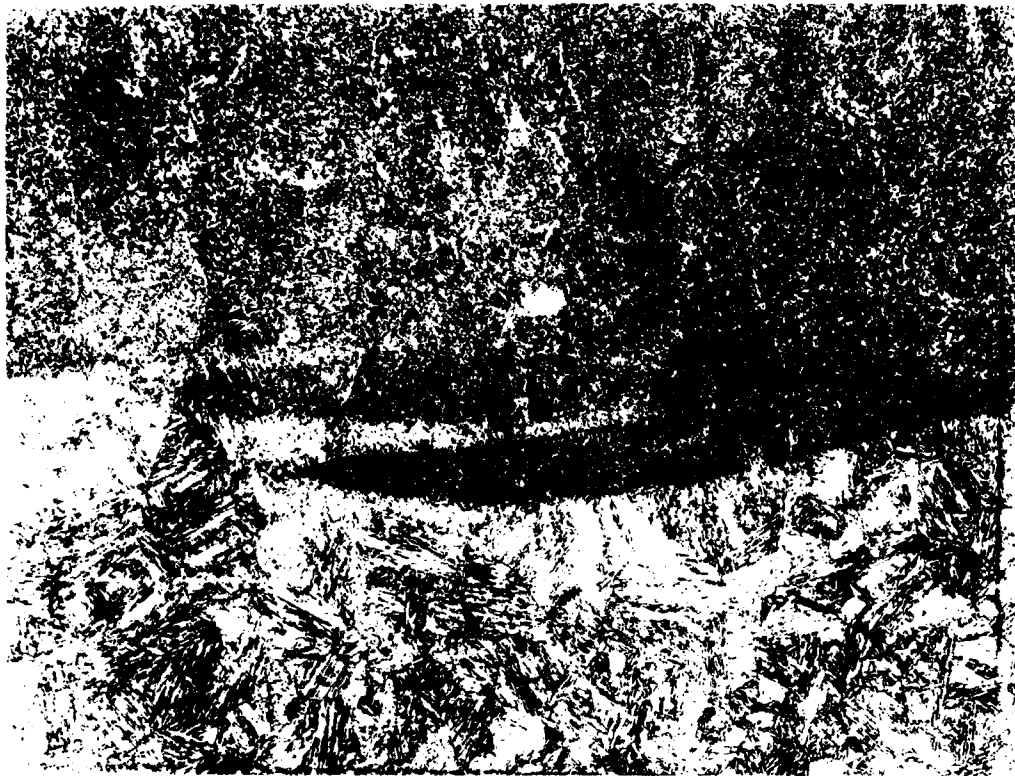
Figure 46. Interleaving between base metal and weld metal at
the fusion line of a Shielded Metal Arc weld.

END
DATE
FILMED
7 84
DTIC
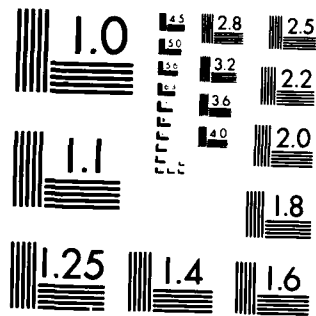
MICROCOPY RESOLUTION TEST CHART
NATIONAL BUREAU OF STANDARDS-1963-A
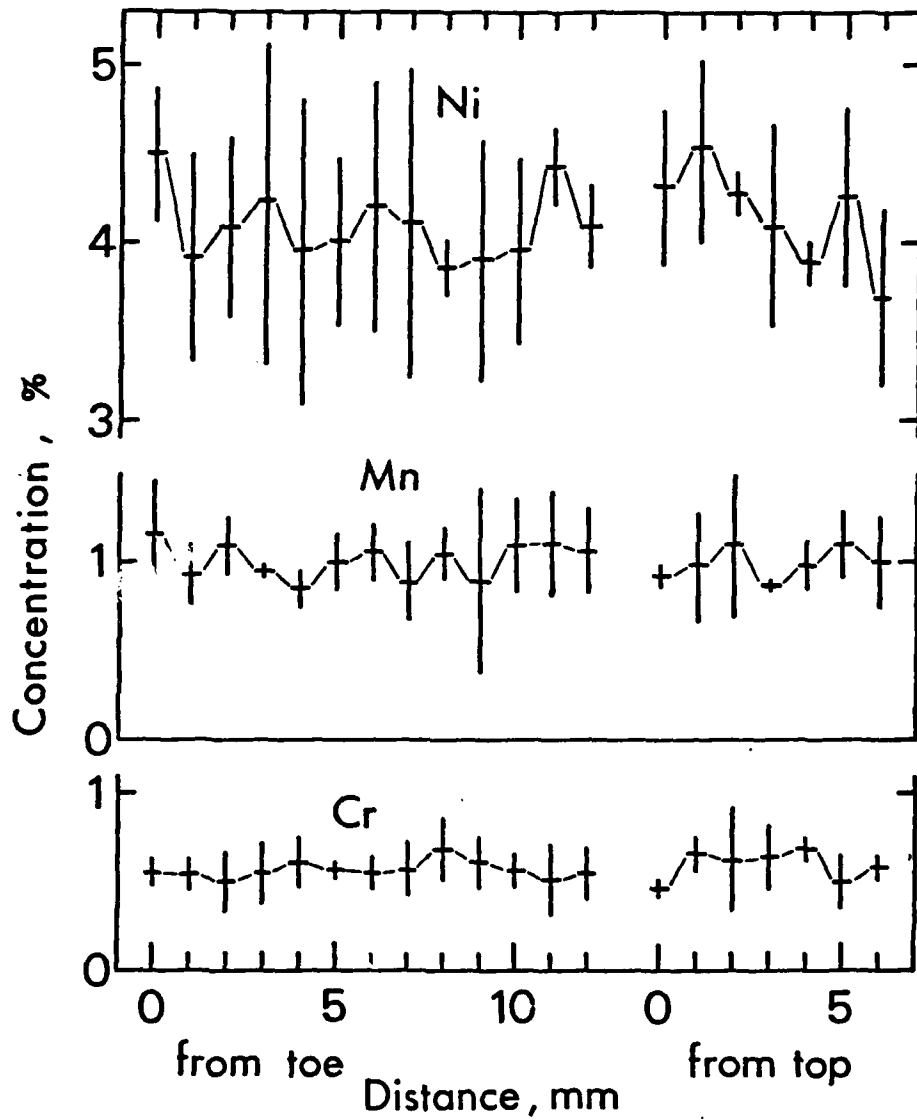
Figure 47. Results of microprobe surveys on conventional E14018 deposit. Bars are 2-sigma limits.
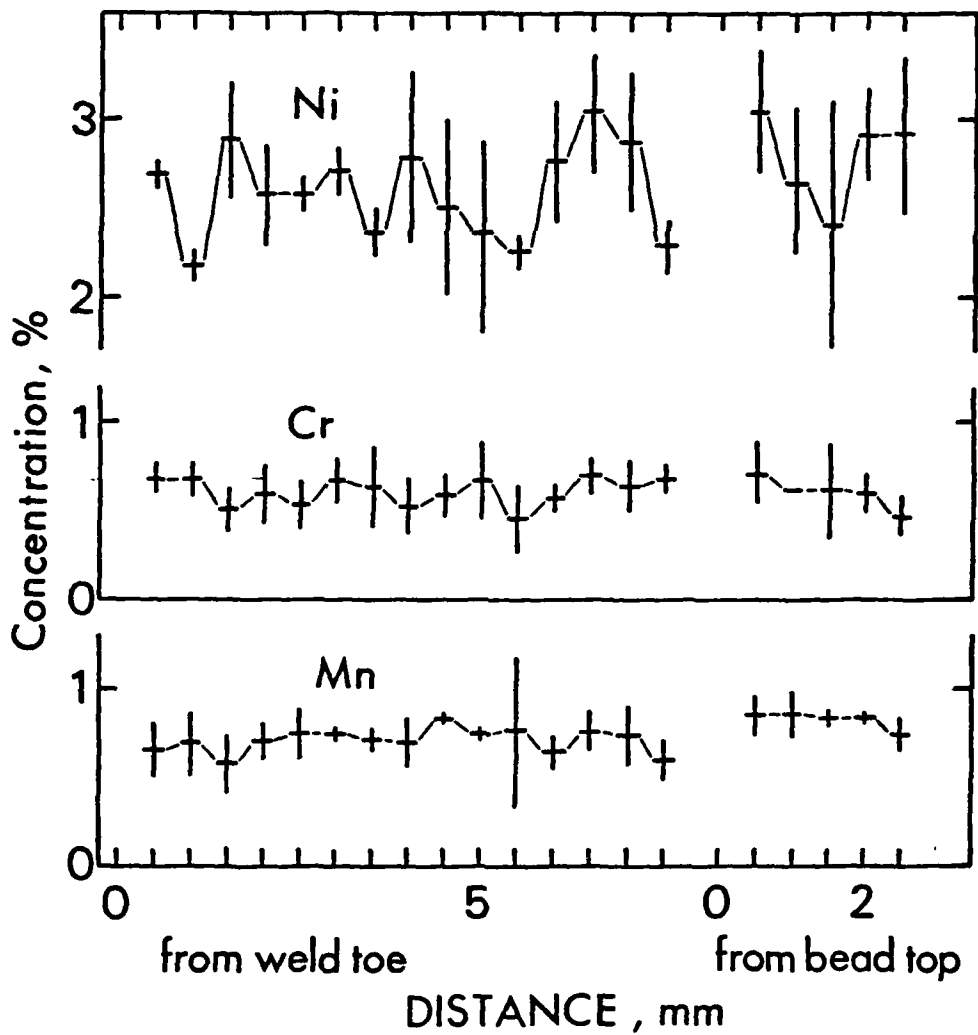
Figure 48. Results of microprobe surveys on ribbon
type electrode deposit. Bars are 2-sigma limits.
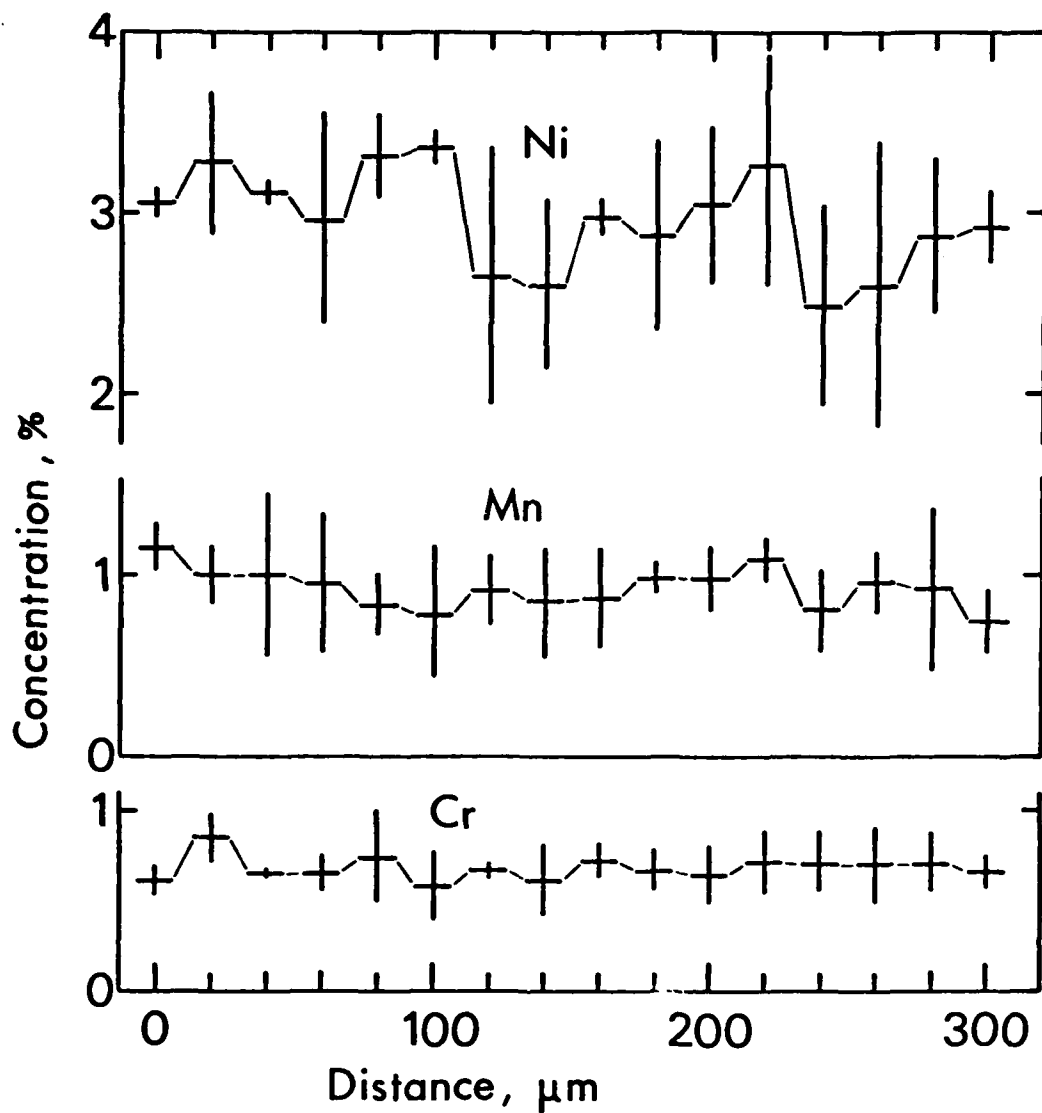
Figure 49. Microprobe traverse across light etching
band in figure 50. Weld produced with ribbon type
electrode. Bars are two sigma limits.
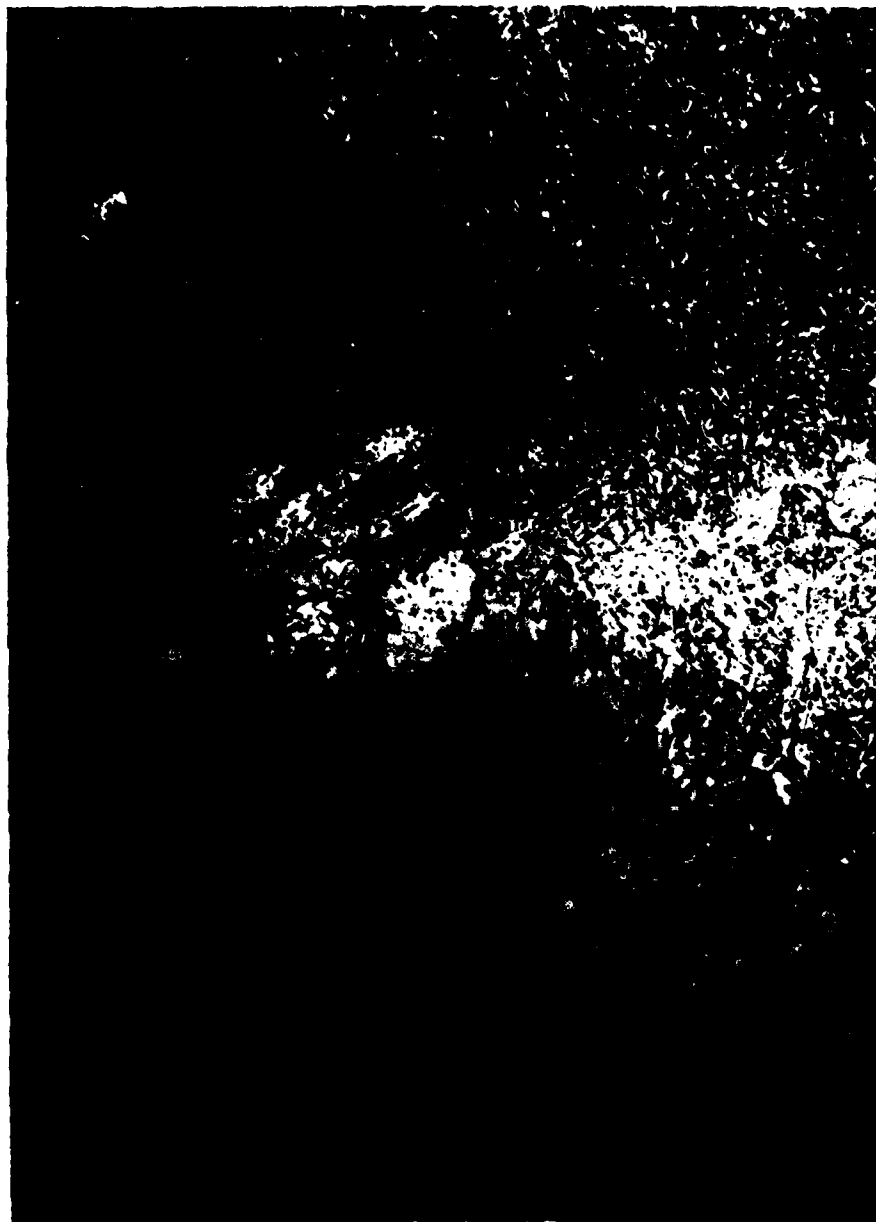
Figure 50. Light etching band in a ribbon type composite electrode weld. Microprobe traverse is shown in figure 49. (200X, 2% Nital)

92
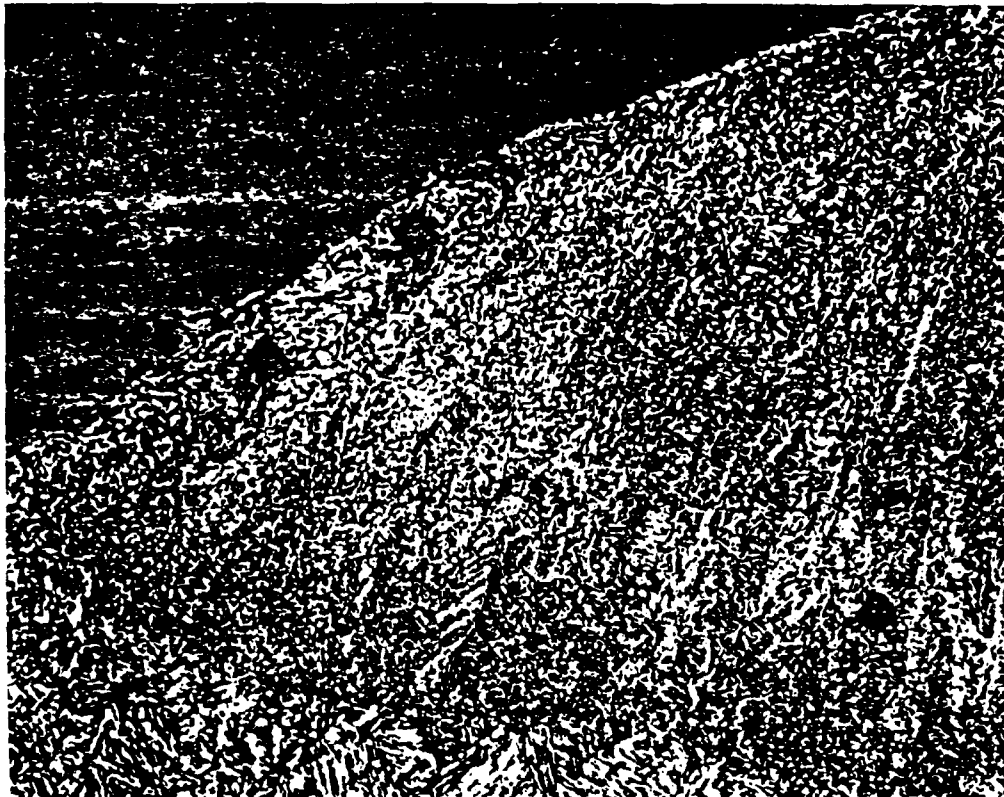
Figure 51. Light etching band at the start of a rib-
bon type composite electrode weld. Microprobe results
are given in table 15. (100X, 2% Nital)

TABLE 15.   SEM X-RAY ANALYSIS OF LIGHT AND DARK ETCHING
AT BEGINNING OF A SHIELDED METAL-ARC WELD

	Light Area	Dark Etching Weld Metal at Weld Center
Cr	0.52 +/- 0.13%	0.62 +/- 0.08%
Mn	0.85 +/- 0.13	1.08 +/- 0.06
Ni	2.56 +/- 0.36	2.47 +/- 0.33

Based on analysis of 100 micrometer square areas, standard of
independently analyzed HY-130 base material.

TABLE 16. MECHANICAL TEST RESULTS

	Yield Strength (psi) 135,000-150,000 @ .2% offset	Ultimate Tensile Strength (psi) Recorded for information only- no requirement	Percent Elongation 14% min.	Percent Reduction in Area Recorded for information only- no requirement	Dynamic Tear (ft-lb)
Requirements for Mil 140S-1 and Mil 14018-M1					@+30F 500
SMAW 1/8" dia. ribbon electrode (.096) J369					@+30F 90 / 140 (mean: 115) @+100F 520 / 570 (mean: 545)
J370	140,450 / 145,560 (mean: 143,000)	145,560 / 152,780 (mean: 149,180)	14.5 / 15.0 (mean: 14.8)	54.7 / 55.8 (mean: 55.3)	
GMAW GMA-01	145,860 / 144,340 (mean: 145,100)	153,380 / 147,960 (mean: 150,680)	5.5 / 2.5 (mean: 3.0)	11.2 / 8.9 (mean: 10.1)	
GMA-02	143,160 / 140,450 (mean: 141,800)	152,180 / 152,180 (mean: 152,180)	17.5 / 16.0 (mean: 16.8)	50.7 / 47.6 (mean: 49.2)	
GMA-04					@+30F 240 / 340 (mean: 290) @+100F 465 / 410 (mean: 487)
SAW SAW-01	140,830 / 141,720 (mean: 141,280)	148,880 / 148,580 (mean: 148,740)	16.0 / 15.5 (mean: 15.8)	58.0 / 55.9 (mean: 56.9)	
SAW-02					@30F 440 / 410 (mean: 425) @+100F 450 / 490 (mean: 470)

Figure 52. 3T bend specimens.

(a) submerged arc (SAW-02)

(b) gas metal arc (GMA-04)

(c) shielded metal arc (SMA-J369)

Figure 53. Failed tensile samples from GMA-02 showing ductile appearance and cup-cone fracture.
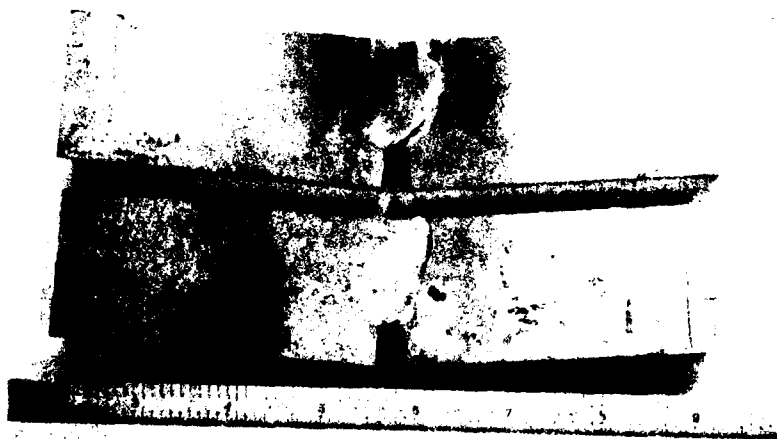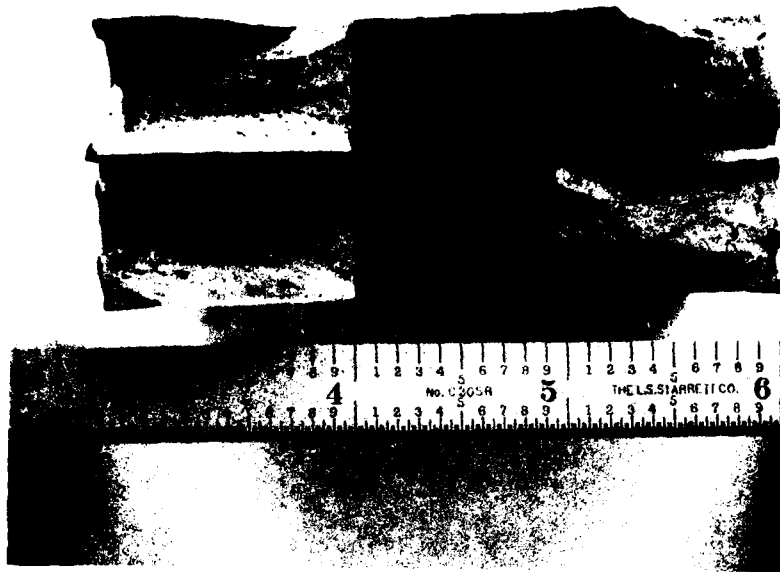
Figure 54. Submerged Arc dynamic tear samples, tested at
+30F (SAW-02)

98
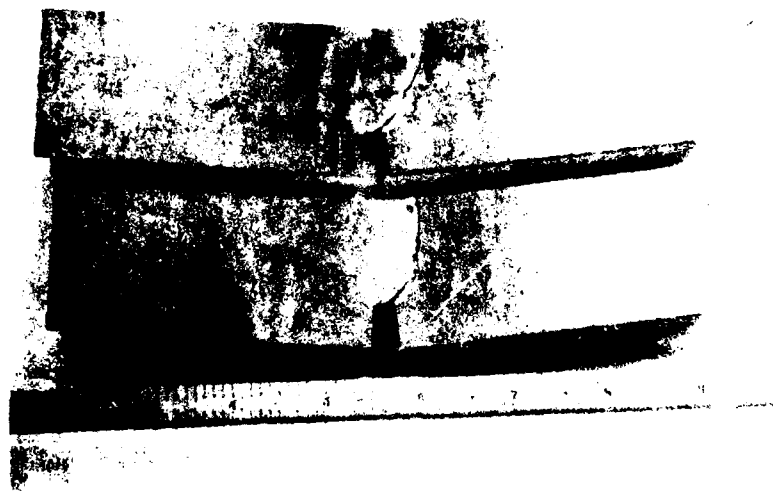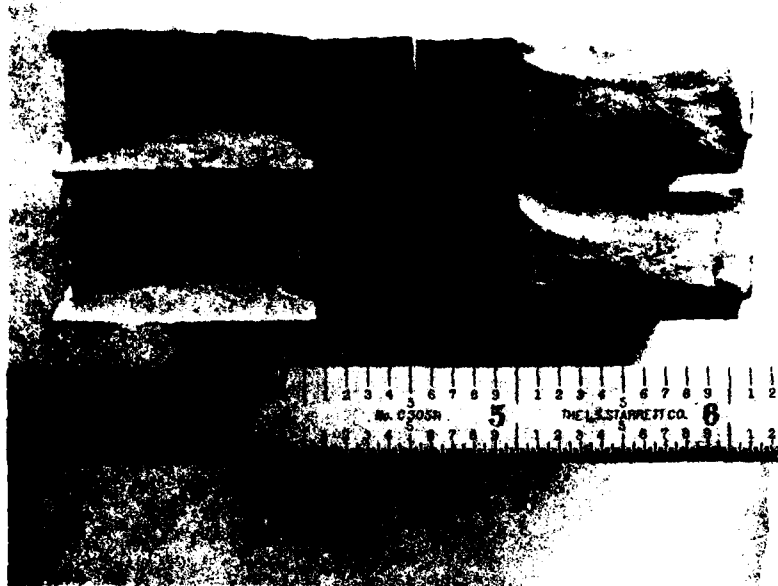
Figure 55. Submerged Arc dynamic tear samples, tested at +100F (SAW-02)

99

however, the absorbed energy rose to a mean of 545 ftlbs indicating that, at 30F the material is in the fracture transition region. It is suspected that impurities (oxygen, sulfur and phosphorus) in the commercial core wire may have caused the transition temperature to increase. No particular effort was originally made to select core wire with specially low impurities.

The GMA weld did not provide as good toughness as expected. At 30F, the mean value was 290 ft-lbs, and additional tests at 100F resulted in a value of 438 ftlbs. This was probably due, again, to the relatively high impurity levels in the deposit. In addition to the shift in transition temperature, high impurity levels can also reduce the upper shelf energy values. Filler materials in the lower strength ranges are much less sensitive to impurities, and produce acceptable properties at much higher impurity levels. This, combined with economic considerations, greatly reduces the demand for (and availability of) low strength fillers with low impurities. One of the major reasons for the selection of the E80S wire was that the impurity levels were much lower than other available wires. Even so, these levels were still above the upper limits for 140 filler materials. For large quantities it would probably be possible to obtain a special heat with low residuals at a reasonable cost.

CONCLUSIONS

This investigation has shown that weld pool filler synthesis is a viable method to produce a desired weld metal composition. The Shielded Metal Arc, Gas Metal Arc and Submerged Arc processes may all be adapted to this technique. While the initial equipment costs are higher, synthesized deposits using "off the shelf" consumables could result in significant savings in the cost per pound of weld wire when compared to single wire systems. This method represents an additional source for hard-to-obtain fillers and also lends itself to filler metal development where a range of compositions may be studied without producing individual heats.

The homogeneity obtained was very good overall, although there were a few inconsistencies. The slight alloy banding in the Composite Shielded Metal Arc deposits was similar to that of conventional E14018 Deposits, indicating a possible solidification effect. However, molybdenum banding observed in E14018 deposits was not detected in the composite welds. This indicates there may be an advantage to adding the alloys in elemental form rather than as ferroalloys. The Gas Metal Arc deposits exhibited some lack of mixing at the penetration finger. This did not seem to have much effect on mechanical properties, and could probably be reduced through further refinement of the technique. The Submerged Arc deposits showed excellent uniformity, and this may have been due to the differences in penetration characteristics when compared to Gas Metal Arc.

The tensile properties obtained were excellent, with all three processes meeting the minimum requirements for yield strength and ductility once the parameters had been optimized. The Submerged Arc process came close to meeting the dynamic tear requirements, while the dynamic tear results for the other processes were not as good. This was thought to be due to high residual element content of the wires used, and could be optimized for all three processes through proper selection of starting materials. In all cases the yield strength was higher than desired, and this was probably a contributing factor to the substandard toughness.

REFERENCES

1. MIL-S-24371A(ships) 1975 Military Specification- Steel Plate, Alloy, Structural, High Yield strength (HY-130) 21 August 1975.

2. MIL-E-24355A(ships) 1975 Military Specification- Electrodes, Welding, Bare, Solid, Manganese-Nickel-Chromium-Molybdenum Alloy Steel for Producing HY-130 weldments for as-welded Applications. 24 October 1975.

3. Heuschkel, J. Weld Metal Composition Control. Welding Journal Research Supplement August 1969. 48:328s-347s

4. Flemings, M. C. Solidification Processing. McGraw-Hill, New York 1974.

5. Savage, W. F., C. D. Lundin and A. H. Aronson. Weld Metal Solidification Mechanics. Welding Journal Research Supplement April 1965 44:176s-181s

6. Gouch, A. J and H. Muir Segrgation of Alloying Elements in MMA Pipeline Welds. Metal Construction March 1981 13:3:150-158

7. Savage, W. F. and E. S. Szekeres Technical Note: A Mechanism for Crack Formation in HY-80 Steel Weldments. Welding Journal Research Supplement

8. Muir, A. R. A Consideration of the Factors Affecting Porosity in Self-adjusting Metal-arc Welds on Mild Steel. British Welding Journal July 1957 4:323-335

9. Warren, D. and R. D. Stout. Porosity in Mild Steel Weld Metal. Welding Journal Research Supplement September 1952 31:406s-420s

10. Meitzner, C. F.and R. D. Stout Microcracking and Delayed cracking in Welded Quenched and Tempered Steels. September 1966 45:393s-400s

11. Woods, R. A. and D. R. Milner. Motion in the Weld Pool in Arc Welding. Welding Journal Research Supplement April 1971 50:163s-173s

12. Erohkin, A. A. A Study of Electrodes With Alloying Elements Added to the Covering and Flux Core. Weld Pool Chemistry and Metallurgy, pp.251-258. The Welding Institute, Cambridge, England 1980.

APPENDIX

WELDING CONDITIONS FOR MECHANICAL TEST PLATES

SHIELDED METAL ARC

Condition	Tensile Test Plate
Current (amp)	110 - 115
Voltage (volt)	22 - 23
Travel Speed (ipm)	4.5 - 5.0
Heat input (KJ/in)	30 - 35
Preheat Temp. F	200 - 225
Interpass Temp. F	200 - 225
Position	Vertical - Up
Filler Metal	0.125" diameter (ribbon composite, .096)

Condition	Dynamic Tear Plate
Current (amp)	130
Voltage (volt)	22 - 23
Travel Speed (ipm)	4.0 - 5.0
Heat input (KJ/in)	35 - 40
Preheat Temp. F	275 - 300
Interpass Temp. F	275 - 300
Position	Flat
Filler Metal	0.125" diameter (ribbon composite, .096)
Post Weld H.T.	350 F for 12 hours

GAS METAL ARC

Condition	Tensile Test Plate	Dynamic Tear Plate
Current (amp)	320	320
Voltage (volt)	25.5	25.5
Travel Speed (ipm)	11	14
Heat input (KJ/in)	44.5	35
Preheat Temp. F	275 - 300	275 - 300
Interpass Temp. F	275 - 300	275 - 300
Position	Flat	Flat
Primary Wire	1/16 inch diameter E 80S-D2	
Speed ipm	176	176
Sec. Wire	0.035 inch diameter Hastelloy X	
Speed ipm	25 - 26	25 - 26
Shielding Gas	Argon - 2% Oxygen, 50 cu. ft/hour	
Stick out (in)	5/8	5/8
Post Weld H.T.	None	350 F, 12 hours

SUBMERGED ARC

Condition	Tensile Test Plate	Dynamic Tear Plate
Current (amp)	400	400
Voltage (volt)	23	23
Travel Speed (ipm)	13.5	16
Heat input (KJ/in)	40.9	34.5
Preheat Temp. F	275 - 300	150 - 175
Interpass Temp. F	275 - 300	150 - 175
Position	Flat	Flat
Primary Wire	1/16 inch diameter L-44	
Speed imp	207	207
Sec. Wire	0.035 inch diameter Hastelloy X	
Speed ipm	24	24
Flux	Oerlikon OP121TT	
Stick Out (in)	1/2	1/2
Post Weld H.T.	350 F for 12 hours	350 F for 12 hours